We are grateful to the referees for their thoughtful comments. We believe the revised manuscript has benefitted greatly from their inputs.

The ***key changes*** are

More prominent discussion of observational limitations, as we have included a separate subsection in the discussions (Reviewers 1 & 2).

Clearer description of the different elevation loss rate estimates, as we more clearly discuss and contrast the sub-seasonal and seasonal, i.e. time-averaged, rates (Reviewers 1 & 2)..

Better balance between main document and supplement, by moving two results-related figures into main document (Reviewers 1 & 2).

Minor changes include

Extended discussion of the slow start to mass wasting (Reviewer 1)

Picking out one slump that is discussed in more detail (Reviewer 1)

Streamlined and harmonized the figures (Reviewer 1)

Improved discussion of polycyclic slump activity (Reviewer 1)

Discussion of the complementarity of fieldwork and remote sensing approaches

Inclusion of recent publications (e.g. Stettner et al. 2018)

Numerous language edits

The changes to the main document and the supplement are described in detail in the replies to the referees.

Reply to Referee 1

> This study uses single-pass interferometry (an idea similar to DEM differencing, but in terms of interferometric phases) from bistatic TanDEM-X data to measure elevation changes at thaw slumps. Based on their results that show temporal evolutions in the summer of 2015 over two large areas in the Arctic (Tuktoyaktuk and Lena Delta), the authors quantitatively pointed out that the surface subsidence over headwalls didn't always track the changes in the input thermal energy, a conclusion that is stated in the title. This is an innovative and interesting work that I deem suitable for publishing in TC. However, I still have some comments for the authors to consider.

We thank the reviewer for the detailed and constructive comments, which we address point by point below. We hope that our modifications will make the manuscript clearer and more complete.

> 1. The authors pushed to the limits of the TanDEM-X data for these two landscape scale studies on individual thaw slumps. Overall, I agree with the authors' strategies and conclusions. The authors may consider adding a summary of the following limits from the data in the discussion session. The first limit is the spatial resolution: the multi-looked dh images have postings of 12 m, corresponding to an area limited of 1 ha, yet only 14% of the slumps are larger than 1 ha (page 8, line 28). Moreover, the analysis or interpretation is not based on individual resolution cells, but on spatially aggregated ones to active parts within each slump. I agree with this spatial-averaging approach. But I suppose this further reduces the number of slumps that can be investigated, simply because the active parts of the chosen slumps must contain several 12-m pixels. Generally speaking, would the overall results and conclusions about "not t consistently energy limited" be biased towards large slumps? Is it possible that small slumps are more likely to be energy-limited? The second limit is the uncertainties and biases. The authors have carried out a detailed analysis on this in section 3.1.2. Spatial aggregation also helps. The third is the limited temporal sampling. The authors produced 4 to 6 data points of temporal elevation changes for their sub-seasonal studies. This is probably the best data one can use for regional-scale mapping, thanks to the 11-day repeat of the TanDEM-X data. But there is a mismatch between the relatively poorly-sampled elevation changes and the daily meteorological changes (e.g., Fig 3). The cluster analysis indeed helps to boost the confidence level, reduce the contamination of local anomalies in individual time series, and reveal the three overall temporal patterns (Fig. 4). C2

We now try to provide a better account of these issues. The potential sampling bias is a good point. We now mention it explicitly in a new subsection in the discussion, along with a brief summary of the limitations of single-pass interferometry. In particular, we acknowledge the limitations imposed by the height precision (e.g. for tracking slump floor dynamics), by the spatial resolution (e.g. for distinguishing headwall retreat from processes on the slump floor), and by the temporal sampling (mentioned in the discussion of rainfall-related processes). We also tried to highlight these issues more prominently throughout the introduction ('the comparatively large measurement noise'), the methods ('As these uncertainties are comparable to the signal magnitude, a detailed uncertainty analysis is required.') and the conclusion (first bullet point).

We cannot quite follow the details of the argument about the slumps that are smaller than 1 ha. Even for smaller slumps (around Tuktoyaktuk, a typical smaller slump is around 0.3 ha in size), the resolution is adequate for resolving those slumps: one pixel is about 100 m^2 (see Sec. 3.1.1.), a 0.3 ha slump is 3000 m^2, corresponding to 30 pixels. Clearly, a better resolution would be preferable.

> 2. The conclusion on "the widespread presence of an insulating veneer of debris or snow on the headwalls" is largely speculative. I understand the authors' logic and agree that this is a possible reason for the inactive phase in June. But I wish the authors can provide more direct evidence for this assertion.

We agree that our interpretation remains speculative because our data cannot separate the two processes that are most likely implicated in the observed subdued activity. These are i) a debris/snow cover and ii) heat flow into the cold slump material, and as i) reduces the energy input into the cold slump, the two are not independent. To cleanly quantify the joint role of the two processes, in-situ observations such as temperature profiles would likely be required. Unfortunately, we could not collect such data in 2015. We plan to instrument several slumps in the Tuktoyaktuk coastlands in 2018 to answer this question.

Despite the uncertainties, it is important to point out that the prevalence of an early-season veneer has been reported regularly by fieldworkers. We cite two relevant papers (Lacelle et al. 2015, Lewkowicz 1987).

To better highlight these limitations, we have extended the discussions by explicitly acknowledging the impossibility of attribution). We also draw attention to it in the conclusions.

> 3. The authors may include a clear, representative slump to illustrate the temporal changes as revealed by the TanDEM-X data, like what is presented in the supplementary materials but for a typical case. I believe this could help the readers better understand the strengths and limitations of the data as well as the key results (time series and elevation loss rate map).

We agree that this is a helpful addition. We have now added the elevation changes at one slump to Fig. 3 (image and time series). It is representative in that its elevation losses are very small at the beginning of summer and then pick up in mid-July. We also refer to it repeatedly in the results and discussions..

> 4. Can the authors present the same sets of results for their two study areas? Namely, maps of slump activities and dynamics (like Fig 2a,b) for Lena River Delta, and map of elevation loss rates (like Fig 6b) for Tuktoyakuk?

We have tried to homogenize the presentation of the results, but slight discrepancies remain. The Lena River Delta (Kurungnakh) region now includes time series of meteorological forcing to make it comparable to the other study regions. The Tuktoyaktuk coastland figure (Fig. 2) now includes a map of the seasonal elevation losses r_s, albeit not the TanDEM-X derived image itself (the slumps would be much too small to see as the extent of the study region is > 100 km), but using a colour-coded point plot. In Bykovsky, by contrast, the slumps are larger and the study area much smaller, so that we can show a map of the elevation changes for the entire study area. The dynamics, which are shown in Fig. 6b) are similar for all slumps (hence no clustering and no separate plot of cluster membership; we now mention this explicitly in the text).

> 5. It's not clear to me how "Time-average elevation loss rates were computed by stacking time series of individual h measurements" (section 3.1.3, page 8). My understanding is that the elevation loss rates are estimated at the middle of subsequent acquisitions (Fig 3). At first, I had to guess that the authors used several pairs that have the same mid epoch but different spans to average (like two pairs day 1-day 14 and day 12-day 34 have the same mid epoch on day 23). But this would produce sparser sampling that what is shown in Figure 3. Then I found this

> description in S.1.1 "The stacked elevation loss rate rs was computed from the time series of estimates assuming a constant rate." Please clarify this stacking method. What is always helpful is to provide a list of images used and interferometric pairs generated and their spatial baselines (in supplementary materials).

We have tried to clean up our descriptions:

- The methods section has been rewritten: in particular, the sub-seasonal rates r estimated from successive image pairs are explicitly contrasted with the stacked seasonal rate estimates r_s
- The caption of Fig. 3 mentions explicitly that we plotted the rate halfway between the two successive image pairs (shown on the horizontal axis)
- The temporal extent is now explicitly mentioned in all captions
- We now explicitly mention the number of TanDEM-X acquisitions in the results as well as that the results belonging to Fig. 3 were computed based on r

> Lastly. I felt that I reviewed two super-long papers: the main manuscript focuses on the key ideas and results centered around thaw slump geomorphology and dynamics as well as their meteorological drivers; and the supplementary material that describes the technical and mathematical details related to the measurements of elevation changes from single-pass interferometry, and clustering analysis (as well as numerous other detailed results). I understand why the authors opted this way of dividing the dense contents into two documents, esp. for TC readers. But I had to constantly go back and forth between these two documents, which greatly disrupted my reading. Practically, I found it is very difficult to include my review comments on the supplementary materials as there are not enough space and no line numbers to refer to. I provide a few comments below. I can give a more detailed review of the supplementary materials in the next round, provided that they are friendlier to reviewers.

We apologize for the omission of line numbers. We are grateful for the comments on the supplement, which we address below.

We are aware of the large amount of information contained in the submission. However, we felt the uncertainty analyses/detailed methods (such as developments of statistical tests) did not warrant a separate submission. At the same time, we feel it is important to describe certain technical aspects like the biases in detail (not least because certain analyses are, as the reviewer rightly contends, close to the technical limits imposed by the technique).

To improve the flow of the paper we have moved results-related figures from the supplement to the main body of the document (cluster statistics and membership). We hope that this facilitates reading the manuscript without recourse to the supplement.

> Page S1 "The stacked elevation loss rate rs was computed from the time series of estimates ..." See my 5 comment above.

We address the description of r_s above.

> Page S2 "such a positive correlation was indeed observed (Fig. S3)". But I have to say that the positive correlation looks weak to me.

Agreed. We now qualify the strength of the correlation in the text as weak.

> Page S7, Table S1: the units for along-track baseline should be m. And what is 'effective' baseline?

To clarify these issues, we have made two changes. We have renamed the quantity to along-track interferometric time lag. The advantage over the spatial baseline is that it is much easier to interpret. We have also cited a relevant paper (Suchandt and Runge; in both the text and the caption) that discusses the concept of effective time separation (or baseline) in detail: loosely speaking it is the time separation so that the along-track phase phi = 2*k*v_los*tau_eff, where v_los is the line of sight velocity of the target. It differs from the standard concept for ATI systems in which one of the antennas is purely passive.

> Figures related: Figure 1e: Lack of vertical scale as the reference in the photo. Readers can have a guess from the caption though.

We have considered adding a scale to the picture itself, but we think that the caption suffices.

> Figure 4, first row plots of normalized rates: clarify how the normalization is done. Why the maxima of normalized rates are not 1?

We now mention that the absolute elevation changes sum to one. This is the same normalization we use in the tests (Eq. S4).

> Figure 4, TDD plot: would the averaged TDD within each period be more consistent with the averaged elevation loss rates than the maximum TDD? I don't expect this would change the increasing trend in TDD though.

The reason we show the maximum TDD is the potential link between the end-of-summer acceleration to a crossing of a thaw depth threshold, which in turn would be related to the maximum TDD. We mention the crossing of a thaw depth threshold in Sec. 5.

> Figure 5a: why the elevation changes rates and their uncertainties are positively correlated?

Good point, to which we do not have a compelling answer. We believe at least two factors to be important. First, larger headwalls tend to have larger volume losses, but they also are prone to certain uncertainty increasing measurement artefacts such as radar shadow, cf. discussion of uncertainties. Second, selection biases will reinforce this effect, as slumps that are, for instance, small and stable would have a high uncertainty and a low volume loss rate, and would thus less likely show detectable activity.

> Figure 6c. Naturally, readers expect to see close-up images for all the four boxes in 6b.

We realize this is not ideal. However, we tried shrinking the insets so we could include all four but found the previous version to be more effective.

> Minor comments:

> Page 1, line 7: during summer *of 2015*

done

> Page 1, line 14: the slump area *and headwall height*

We have replaced slump area with headwall height

> Page 1, line 20: One of the motivations of this study is to advance geomorphic modeling/prediction of thermokarst. But the two papers cited (Lewkowicz, 1987; Günther et al., 2015) are both observational work, not modeling work. Please provide more situation references.

We have included Westermann et al. as an example for a mechanistic (as opposed to data-driven) model

> Page 2, line 5: add a comma before "which we here .."

done

> Page 3, line 15: 'rate-limiting' is used interchangeably as 'energy-limiting'. To avoid possible confusion, change it to 'energy-limiting' or 'energy-limited'.

done (but slight rephrasing)

> Page 3, line 16: the temporal signature *of volume loss*

done

> Page 3, line 23: extra heat is used to heat and thaw the cold active layer as well.

Good point. The next sentence now reads: 'Early summer mass wasting may also be subdued because the incoming energy is used to warm the cold permafrost to the melting point before ablation can set in'

> Page 4, line 15: Shuttle Radar Topography Mission (first letters are capitalized)

done

> Page 5, line 23: replace 'tundra lakes' with thaw lakes or thermokarst lakes

We have replaced 'tundra lakes' with 'lakes'; the reason for not specifying the lakes further is their geological diversity (glacial processes have likely contributed to shaping especially some of the larger lakes)

> Page 6, line 29: products (plural form)

Rephrased sentence

> Page 6, line 30: what is the source of the input DEM?

The input DEM was derived from TanDEM-X data acquired before or during the Science Phase.

> Also page 8, line 32: provide more information about the pre-disturbance DEM.

We now provide details on the DEM (MVAP DEM, 2008, Northwest Territories Centre for Geomatics) in the text.

> Page 7, line 12: explain what is isotropic seasonal subsidence and why it is expected to be similar at the spatial scales of your interest.

We now refer to the subsidence associated with top-down thaw as permafrost thaw subsidence and provide a citation. The attribute ‘isotropic’ is commonly employed to describe the spatially uniform nature of the subsidence.

> Page 8, line 3: how small? Can add the estimated magnitude as presented in the supplementary materials.

2 cm vs. 30-60 cm; now both sets of numbers are included in the main document, as is a reference to the appropriate Fig. in the supplement

> Page 9, line 3: ‘earlier generation’ implies multiple cycles, and more implicitly that the life cycle is about 10 years by comparing images from 2004 and 2016 . Somewhere earlier, best in the introduction, this can be mentioned.

We have added two sentences on polycyclic activity in the introduction

> Page 11, line 13: Fig. S8*c*, to be more specifically.

Done; the figure has been moved to the main document.

> Page 11, line 29: “two peaks in mid-July and mid-August. But Fig 3d shows at least four peaks during this period. Please clarify what are the two peaks.

The two peaks refer to the restricted time period shown in Fig. 4; we now reference Fig. 4 explicitly

> Page 15, line 12: “suggests a strong influence of downstream sediment dynamics..” please elaborate more on this.

Done, but in the discussions. There, we discuss sediment supply driven by mass wasting at the headwall, and sediment evacuation from the scar zone. We also mention that our observations are insufficient for resolving these processes.

> Page 16, Figure 5b shows that elevation loss rates are correlated with the relief. Any comments?

We mention it in the text but do not discuss it in detail. Apart from the direct increase of volume losses with headwall relief that would be expected if the planimetric backwasting was constant, there is also evidence for increased backwasting at larger slumps (Lacelle et al. 2015), albeit at longer time scales.

> Page 18, delete sentences starting from line 32 to the end of the paragraph. Same sentences appear earlier (starting from line 23). Copy/paste mistake.

done

> Page 19, line 10: change ’effect increased’ to ‘increase’

done

Reply to Referee 2

> The paper " Sub-seasonal thaw slump mass wasting is not consistently energy limitedat the landscape scale" is using repeated single-pass InSAR data from the TanDEM-Xmission to assess the analyze the sub-seasonal thaw slump activity in two two ice-rich study sites during summer 2015. The analyzed data indicates that mass wasting in the assessed areas is not always energy limited at the landscape scale. The level of detail to which the data sets are analyzed (both scientifically and technically) is impressive.The results achieved are manifold and highly valuable for this field of research. Overall,this is an impressive paper that definitely warrants publication in this journal.

We are grateful to the referee for their helpful and constructive comments. We believe that thanks to the reviewer's input the clarity and quality of the revised manuscript have improved.

> That being said, I have the following comments/concerns and suggestions whose consideration might further improve the value of this paper:
>
> Main (general) comments:
>
> 1. The paper is well written and both the description ofapplied methods as well as the discussions of achieved results are clear. However,the split of the material into "main paper" and "supplemental information" is not always appropriate and hinders the reading and comprehension of the material. While I understand the motivation between splitting the material into a more scientific discussion and a more technical analysis, some of the figures that are currently in the supplemental content might be better placed into the main paper to improve clarity. For instance, FigureS.19 provides a much better view of the associations between headwall elevation loss rates and slump characteristics than Figure 5b. Both figures should be grouped together and discussed together. Other figures that I would prefer in the main paper are S8, S10, and S18.

We hope we have now struck a better balance between the main document and the supplement. We have moved Fig. S8 and S18 in adapted form into the main body of the manuscript. The reason for including these two figures is that they deal with the process-based results (focus of the paper), whereas Fig. S10 is more to do with technical issues. The reason for not including S19 is that we focus on the sub-seasonal mass wasting, whereas S19 deals with longer time scales. We believe Fig. 5b provides sufficient information for our purposes; in particular, the regression analysis accounts for the fact that the explanatory variables like aspect and area are correlated. In addition, we have tried to provide a better link between the main document and the supplementary material.

> 2. A major component that is currently missing in the paper is a discussion of the appropriatenessof the used remote sensing data for the research at hand. I would contest that the characteristics of currently available remote sensing data such as TerraSARX significantly limit the information that can be extracted about thaw slump dynamics. From my point of view, the following limitations exist:
>
> 2.1 Temporal sampling: The sampling rate of 11 days seems borderline sparse given the high temporal dynamics of confounding processes such as precipitation and radiation inputs. Despite significant day-to-day variably, very little change remains when these variables are averaged over the 11-day period, making an assessment of associations difficult.
>
> 2.2 Spatial sampling: As acknowledged in various places in the paper, the 12m resolution of the InSAR-derived DEM data does not allow for a direct comparison between model outputs and surface lowering as sub-pixel variations give rise to an unknown and spatially varying scaling factor. Higher resolution would significantly improve the reliability of the remote sensing data as well as the conclusions that can be drawn based on these data.

> 2.3 Accuracy of surface lowering measurements: While the achieved measurement accuracy (60cm) is impressive, it is still a limiting factor especially for an analysis of processes in the scar zone, where height change rates are at the noise level.
>
> It would be great to see an additional sub-section in Section 5 "Discussion" that is dedicated solely to the appropriateness of the used remote sensing resources and to suggestions for future sensors that could provide more insight into this field of research.

We agree with the referee and have tried to paint a clearer picture. To this end, we have added an additional subsection in the discussion. There we briefly summarize the key limitations, while also highlighting the technique's advantages and contrasting them with complementary tools such as LiDAR. We also acknowledge the uncertainties and biases throughout the introduction (e.g. 'the comparatively large measurement noise'), the methods ('As these uncertainties are comparable to the signal magnitude, a detailed uncertainty analysis is required.') and the conclusions (first bullet point).

We also pick up on existing and future observing systems that hold promise, drawing attention e.g. to the potential of higher radar frequencies such as Ku band, as they can achieve higher spatial resolutions and accuracies.

> 3. I was a bit confused by the use of the stacked elevation loss rate data (r_s) in thepaper. While it is technically clear how r_s is calculated, it is not disclosed how many multi-temporal samples were used to calculate r_s. Furthermore, is it not entirely clearfor which individual analyses r_s was actually employed. From my reading, I found that r_s finds very limited application in the paper and was used only once to analyze the spatial variability of the volume losses in the second half of summer. Instead, I am assuming that the elevation loss values in Figures 3 and 4 were not temporarily averaged, even though this is not clearly stated in the paper. I would appreciate a clearer statement about the use of the parameter r_s in this paper.

We have better highlighted the temporal extent of the elevation loss rate observations throughout the manuscript. The temporal extent is now explicitly mentioned in all captions, and we have also clarified the result sections (e.g. mentioning also the number of TanDEM-X acquisitions, and highlighting that Fig 3 refers to non-averaged rates computed from successive image pairs). Finally, we have slightly rewritten the description of the computation of r_s in the methods, highlighting its purpose (visualization, spatial comparison; Fig. 5) and contrasting it with the computation of the subseasonal rates between successive image pairs, which we now refer to as r throughout the manuscript.

> Minor (specific) comments:
>
> 1. Page 4, line 16: Please add the following reference to the sentence ending in "in volcanology and glaciology": Kubanek J., Westerhaus, M., & Heck B. (2017). TanDEM-X time series analysis reveals lava flow volume and effusion rates of the 2012–2013 Tolbachik, Kamchatka fissure eruption. Journal of Geophysical Research: Solid Earth, 122, 7754–7774. https://doi.org/10.1002/2017JB0 143 092.

done

> Page 18: Repeated identical statements seem to appear (compare lines 20 – 27and lines 29 – line 2 on page 19). Please fix.

done

Sub-seasonal thaw slump mass wasting is not consistently energy limited at the landscape scale

Simon Zwieback[1,2], Steven V. Kokelj[3], Frank Günther[4], Julia Boike[4], Guido Grosse[4], and Irena Hajnsek[2,5]

[1]Department of Geography, University of Guelph, Guelph, Canada
[2]Department of Environmental Engineering, ETH Zurich, Zurich, Switzerland
[3]Northwest Territories Geological Survey, Government of Northwest Territories, Yellowknife, Canada
[4]Periglacial Research, Alfred Wegener Institute, Potsdam, Germany
[5]Microwaves and Radar Institute, German Aerospace Center (DLR), Wessling, Germany

Correspondence to: Simon Zwieback (zwieback@uoguelph.ca), Irena Hajnsek (hajnsek@ifu.baug.ethz.ch)

Abstract. Predicting future thaw slump activity requires a sound understanding of the atmospheric drivers and geomorphic controls on mass wasting across a range of time scales. On sub-seasonal time scales, sparse measurements indicate that mass wasting at active slumps is often limited by the energy available for melting ground ice, but other factors such as rainfall or the formation of an insulating veneer may also be relevant. To study the sub-seasonal drivers, we derive topographic changes from single-pass radar interferometric data acquired by the TanDEM-X [...]satellites. The estimated elevation changes at 12 m resolution [...]complement the commonly observed planimetric retreat rates by providing information on volume losses. Their high vertical precision (around 30 cm), frequent observations (11 days) and large coverage (5000 km2) allow us to track [...]mass wasting as drivers such as the available energy change during [...]the summer of 2015 in two study regions. We find that thaw slumps in the Tuktoyaktuk coastlands, Canada, are not energy limited in June, as they undergo limited mass wasting (height loss of around 0 cm/day) despite the ample available energy, [...]suggesting the widespread presence of an early-season insulating snow or debris veneer. Later in summer, height losses generally increase (around 3 cm/day), but they do so in distinct ways. For many slumps, mass wasting tracks the available energy, a temporal pattern that is also observed at coastal yedoma cliffs on the Bykovsky Peninsula, Russia. However, the other two common temporal trajectories are asynchronous with the available energy, as they track strong precipitation events or show a sudden speed-up in late August, respectively. The observed temporal patterns are poorly related to slump characteristics like the [...]headwall height. The contrasting temporal behaviour of nearby thaw slumps highlights the importance of complex local and temporally varying controls on mass wasting.

1 Introduction

Thaw of ice-rich permafrost, termed thermokarst, has widespread impact on terrain, local ecosystems and the global climate, but the processes that control its [...]rates remain poorly understood (Grosse et al., 2011; Kokelj et al., 2015). High-frequency observations of terrain modification are necessary to elucidate the drivers of thermokarst and to develop [...]models for simulating permafrost degradation in a changing climate [...](Lewkowicz, 1987; Günther et al., 2015; Westermann et al., 2016). The

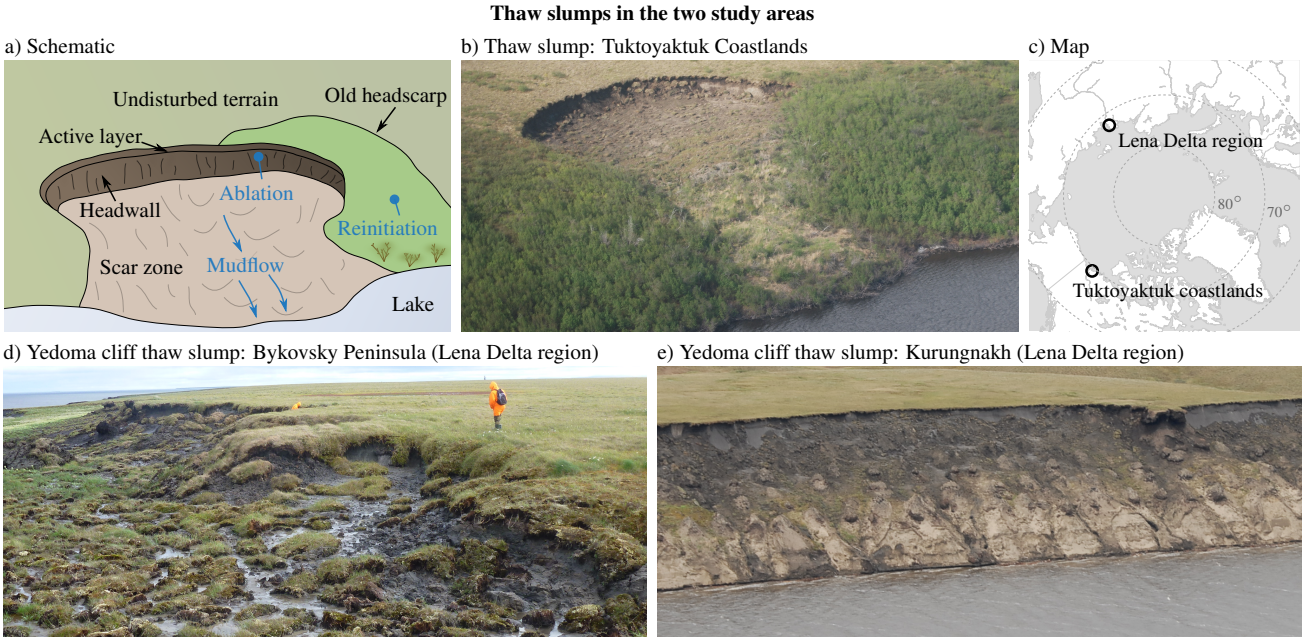

Figure 1. a) Schematic of a thaw slump labelling features in black and processes in blue. b) Retrogressive thaw slump in the Tuktoyaktuk coastlands surrounded by relict, now densely vegetated scars on either side (by S. Zwieback). c) Map of the study regions. d) Headscarp of an elongated cliff thaw slump along Bykovsky's coast (by G. Grosse). e) Thaw slump along the east coast of Kurungnakh (by J. Boike). Note the clearly visible ice-poor sand unit in the lower half of the approximately 30 m-high exposure down to the river level.

sub-seasonal dynamics of thermokarst are also important because they have a direct impact on the local hydrology, biogeochemistry and sediment budget [...](Bowden et al., 2008; Kokelj et al., 2013). In particular, the seasonal timing and magnitude of the thaw-induced mobilization of organic carbon and nutrients influence their lateral transport and chemical fate, and hence the type and magnitude of greenhouse gases released [...](Littlefair et al., 2017; Vonk and Gustafsson, 2013).

Rapid permafrost degradation in ice-rich regions is associated with characteristic landforms. Depending on the topographic position, these are shaped by a wide range of physical processes, which we here include under the umbrella term thermokarst. In flat to gently rolling terrain, thermokarst can be closely coupled to changes in local hydrological conditions, with impoundment of water leading to the formation of thermokarst pits, lakes and wetlands [...](Jorgenson, 2013). On [...]steeper terrain, water also plays a key role in initiating or enhancing thaw degradation in landforms such as thermo-erosional gullies [...]and thaw slumps (Balser et al., 2014; Kokelj et al., 2015). In this paper we focus on thaw slumps[...], which develop when icy sediments are exposed [...]in a steep ice-rich headwall (Fig. 1). [...]As the headwall retreats upslope a low-angled scar zone or slump floor develops. Thaw slumps commonly [...]form adjacent to streams, lakeshores or coastlines where thermal, fluvial and coastal erosion can initiate these disturbances by exposing ice-rich permafrost (Jorgenson, 2013; Lantuit and Pollard, 2008).

Thaw slumps are shaped by thermal, hydrological and mechanical processes over their entire life cycle from initiation to stabilization. Once initiated, active thaw slumps can [...]grow upslope by several metres per year (Lantuit and Pollard, 2008)

as the headwall retreats into the upslope terrain (Fig. 1). Headwall retreat is linked to energy flux (Lewkowicz, 1987), and processes in the scar zone. The mass wasting at the headwall releases meltwater and sediment, which [...]accumulates at the base of the headwall as a saturated slurry and must be removed via [...]downslope fluidized flow in order for backwasting to proceed unabatedly (Kokelj et al., 2015). If accumulated material insulates the ice-rich permafrost or if the headscarp retreats into ice-poor terrain, the thaw slump can stabilize (Lacelle et al., 2015). The [...]accumulation and transport of sediment are coupled to the hydrological conditions, as meltwater and thawing debris typically form a saturated slurry in the slump scar zone [...](Burn and Lewkowicz, 1990). Depending on the water content as well as the sediment input, slope and material properties, this can be a zone of net accumulation or of net volume loss. Net accumulation occurs when the sediments cannot be removed sufficiently quickly: close to the headwall, buttresses of accumulated material can protect the ground ice and reduce retreat rates (Lacelle et al., 2015). Conversely, downslope removal of thawed material at the foot of the headwall can accelerate retreat by exposing ice-rich soil and by increasing the local relief (Kokelj et al., 2015). Thermal processes in the scar zone can also help sustain thaw slump activity by effecting height losses, which are caused by the melting of ground ice in the warm scar zone (Burn, 2000). Many of these same processes that reinforce mass wasting are also central to re-initiating thaw slump activity within stabilized slumps (Kokelj et al., 2009). Such slumps are called polycyclic, as re-initiation results in the formation of a new, actively ablating headwall.

The most important processes in driving headwall mass wasting is the ablation of ground ice. To melt the ground ice at the aerially exposed headwall, energy is required. Ablation increases with insolation and air temperature, as the key terms in the surface energy balance are the radiation input and the turbulent exchange with the atmosphere (Lewkowicz, 1987). If [...]the mass wasting is limited by the available energy, the sub-seasonal rates of volume losses will track the incoming radiation and air temperature. On sub-seasonal timescales of days to weeks, the temporal signature of volume loss is typically steady and slowly declining towards the end of summer (Lewkowicz, 1987). Despite the recognized importance of this process, the prevalence of energy-limited mass wasting has not been assessed at the landscape scale, thus limiting the skill of current thermokarst predictions.

Headwall mass wasting is not always energy limited, and such conditions may be detected using observations of sub-seasonal volume losses. One such exception occurs when an insulating veneer protects the ground ice, thus slowing down volume losses (Kokelj et al., 2015). Such an insulating cover, principally derived from the thawing sediments themselves, as well as from late-lying snow, commonly persists in early summer (Kokelj et al., 2015; Lacelle et al., 2015). Early summer mass wasting may also be subdued because the incoming energy is used to warm the cold permafrost to the melting point before ablation can set in. A separate agent that can govern mass wasting rates is the availability of liquid water from melting ground ice, snowmelt or precipitation (Lantuit and Pollard, 2008). Intense precipitation events may accelerate mass losses in the headwall area in some slumps, both via the removal of debris on or at the base of the headwall, and by water supplying additional energy (Burn and Friele, 1989; Barnhart, 2013; Kokelj et al., 2015). As the additional water input can also liquify the sediments in the scar zone and induce downslope flow, thus lowering the base level for erosion and facilitating the evacuation of the headwall area, precipitation can also feed back positively on headwall mass losses via scar zone processes. Finally, failure related to mechanical instabilities is an important mass-wasting process (Lewkowicz, 1987). Mechanical failure is common when the

base of a permafrost exposure is temporarily in contact with open water, the strong thermal and mechanical influence of which (thermo-abrasion) leads to undercutting, niche formation and subsequent block failure (Wobus et al., 2011). On coastal cliffs, niche formation is closely tied to open water conditions and sea temperatures. It [...]sets in later than energy-limited ablation but can remain effective for longer in autumn (Günther et al., 2015): its prevalence can thus be [...]detected based on a late-summer continuation or speed-up in elevation losses. All three processes have been previously observed in field studies, but little is known about their prevalence and spatial association, as landscape-scale observations of the sub-seasonal mass loss dynamics have up to now not been available.

To study the sub-seasonal dynamics of thaw slump mass wasting, we use synoptic measurements of topographic changes with a nominal temporal repeat period of 11 days. [...]Our estimates of topographic changes are obtained from repeated topographic observations using the radar remote sensing technique single-pass interferometry (Bamler and Hartl, 1998). By repeated application of single-pass measurements, time series of the topography and hence topographic changes can be derived[...]. Repeated observations of two permafrost regions with high ground ice content were made by the TanDEM-X satellite pair in the Science Phase (June - August 2015). The frequent acquisitions every 11 days, the high precision of 20-40 cm and the planimetric resolution of 12 m make this data set an excellent opportunity to study the sub-seasonal dynamics of rapid permafrost degradation.

Single-pass interferometry is a promising technique for observing thaw-induced topographic changes on the landscape scale. While it has not been employed in permafrost environments, the technology is mature, as evidenced by the widespread use of the digital elevation models obtained from the [...]Shuttle Radar Topography Mission or TanDEM-X, or the application of such data for quantifying temporal changes in volcanology and glaciology [...](Krieger et al., 2007; Kubanek et al., 2017). The ability to cover large areas and to do so frequently are key advantages over [...]in-situ measurements[...], photogrammetry and LiDAR (Günther et al., 2015; Jones et al., 2013; Obu et al., 2016). A further advantage is that reliable height measurements can also be made when the soil moisture changes and when the surface structure is disrupted – a common occurrence in rapid mass movements. This is in contrast to the closely related technique differential radar interferometry, which is capable of providing synoptic estimates of more subtle elevation changes associated with seasonal and secular thaw subsidence (Liu et al., 2015; Zwieback et al., 2016). Single-pass data, by contrast, are typically not sensitive enough to capture these slow processes over yearly time scales, but instead are ideal for more rapid thermokarst phenomena.

Here, we pursue two objectives:

1. to derive synoptic estimates of topographic changes and their uncertainty in two ice-rich permafrost regions in the Northwest Territories, Canada, and in the Sakha Republic, Russia (around 5000 km^2) using TanDEM-X data acquired during the Science Phase in 2015

2. to analyse the sub-seasonal dynamics of topographic changes at slump headwalls and their variability between features with the aim of attributing the observed patterns to potential drivers

Our guiding hypothesis is that the volume losses are governed by the ablation of ice, and hence limited by the available energy. To test this hypothesis on time scales of one to several weeks, we compare the observed temporal dynamics to the energy

available for melting ice, which we estimate using a model driven by ground measurements and additional satellite data. [...]Despite the comparatively large measurement noise, significant deviations from energy-limited dynamics are common during the entire thaw period. To attribute these deviations to additional controls, we compare the sub-seasonal fluctuations of mass losses to potential drivers such as precipitation and insulation by snow based on the distinct temporal signatures of these drivers.

2 Study areas

The two study areas are underlain by continuous ice-rich permafrost, and they are locally affected by hillslope thermokarst. The Tuktoyaktuk coastlands in the Mackenzie Delta region in the Northwest Territories, Canada (Fig. 1), are a glacially shaped landscape that contains areas rich in massive ground ice, where retrogressive thaw slumping is common along lake shores (Burn and Kokelj, 2009). Conversely, the Lena River Delta area, northern Yakutia, Russia, was not glaciated. Our data cover two sites in this region, both of which are characterized by extensive yedoma uplands that are underlain by fine-grained, ice-rich Pleistocene deposits. Their very high total ground ice content of up to 90% by volume makes them vulnerable to rapid coastal and river bank erosion and thaw slumping (Wetterich et al., 2008). In summary, the two study areas provide contrasting climatic conditions [...]and geological histories for analysing the sub-seasonal dynamics of thaw slump activity.

The Tuktoyaktuk coastlands [...]were covered by two crossing TanDEM-X orbits that mainly [...]extended in the north-south direction (>100 km), yielding a total area of 4500 km^2. [...]Climatic conditions change along a steep gradient from Inuvik in the south to [...]Tuktoyaktuk on the Beaufort Sea coast [...](Burn and Kokelj, 2009). The southern part of the study area is about 3 degrees warmer in summer than the north (mean July temperature of 14.1 °C in Inuvik vs 11.0 °C in Tuktoyaktuk (can, 2017), whereas the temperature is more uniform in winter. Annual precipitation decreases from 240 mm in the south to 161 mm in the north. The vegetation reflects the climatic gradient, as forest transitions to shrub tundra. The transition zone is characterized by a northward decrease in the density and height of tall shrubs. The gradients in climate and vegetation combine to shape the ground thermal regime, as the minimum near-surface ground temperature decreases from about -3°C in the south to -7°C in the north (Kokelj et al., 2017b).

Retrogressive thaw slumps can be abundant where the relief position and surficial geology are favourable (Fig. 1). They almost exclusively occur in immediate proximity to [...]lakes, which are widespread [...]throughout the study area (Kokelj et al., 2009). The surficial geology varies from hummocky moraine in the south to an increasing proportion of lacustrine plains in the north, interspersed with [...]hummocky moraine and glaciofluvial deposits, both of which may host massive ground ice [...](Aylsworth et al., 2000; Kokelj et al., 2017a). Thaw slumps can grow to areas exceeding several hectares. Headwall heights can reach up to about 15 m, depending on geology and topography (Kokelj et al., 2009). In addition to the mass wasting at thaw slumps, areas of notable slope erosion also occur along the Beaufort Sea coast (Wolfe et al., 1998), and in ice-poor sandy bluffs exposed at large water bodies such as the Eskimo lakes.

The second study area, the Lena River Delta area in north-east Siberia, consists of two sites (Fig. 1). The first site, the Bykovsky Peninsula, is located southeast of the delta close to the harbour town of Tiksi on the Laptev Sea coast. The climate

is subpolar, with mean monthly temperatures varying from -31 °C in February to 8 °C in July in Tiksi (Günther et al., 2015). Geologically, it is characterized by very ice-rich yedoma uplands consisting of thick Pleistocene deposits, interspersed with thermokarst lakes and drained thaw lake basins (alases) (Grosse et al., 2007; Schirrmeister et al., 2017). The Bykovsky Peninsula is subject to continual coastal erosion both along yedoma and the alas coasts (Lantuit et al., 2011). Yedoma uplands that are exposed along the coast form elongated retrogressive thaw slumps (Günther et al., 2013). The upper part of these bluffs, whose height can exceed 40 m, consists of a vertical icy headwall (Fig. 1d). Below the slump headwall, the slopes are more graded but still comparatively steep, shaped by the balance between sediment supply and removal along the bluff. [...]

Kurungnakh Island is located in the southern central Lena River Delta, Russia, around 120 km west of the Bykovsky Peninsula. Its location further inland is associated with slightly colder February air temperatures (-33 °C) and slightly warmer July air temperatures (10 °C, Boike et al. (2013)). The part of Kurungnakh we focus on is also largely covered by yedoma sediments (Morgenstern et al., 2011). Along its eastern margin, bordering the Olenyekskaya Channel, the yedoma sediments (around 25-30 m thick) and the underlying ice-poor fluvial sands form steep cliffs of up to 40 m height above river level (Wetterich et al., 2008; Kanevskiy et al., 2016), see Fig. 1e. In addition, thaw slumping also occurs on slopes surrounding to thermokarst lakes within alases (Morgenstern et al., 2011).

3 Methods & Data

3.1 Height changes and rates from interferometry

3.1.1 Estimating height changes

TanDEM-X bistatic image pairs acquired during the Science Phase 2015 (June to August) served as input for the topographic mapping. The image pairs were acquired with particularly large across-track baselines corresponding to heights of ambiguity of 8–14 m, with which height precisions of better than 0.5 metres can be achieved (Tab. S1). The topographic information was derived from the Coregistered Single-look Slant-range Complex (CoSSc) products. They have a native planimetric resolution of around 3 m, depending on the study area (Tab. S1), which was reduced to 10-12 m during the interferometric processing.

Estimates of topographic changes Δh were derived from time series of TanDEM-X CoSSc image pairs. [...]Topographic changes were computed between successive image pairs that are usually separated by 11 days; the corresponding elevation loss rates (cm/day) are referred to as sub-seasonal rates r. To also characterize the seasonal, time-average elevation loss rates, we stacked the time series of individual Δh [...]measurements and computed the stacked elevation loss rate r_s using generalized least squares. r_s lends itself to spatial analyses and visualizations.

The interferogram for every CoSSc image pair was formed [...]by standard methods (range spectral filtering, removal of the flat earth/topographic phase from the input [...]EM, multilooking) and this time series was co-registered (Bamler and Hartl, 1998). [...]We then directly differenced consecutive interferograms. Our rationale was that the baselines were essentially constant for all acquisitions, so that the differencing of interferograms yielded a direct estimate of Δh and phase unwrapping was greatly facilitated. The differencing of interferograms m and n [...]yielded a phase difference $\Delta\phi = \phi_n - \phi_m$ which

contains the required information about the height difference $\Delta h = h_n - h_m$

$$\begin{aligned}\Delta\phi &= k_{z,n}h_n - k_{z,m}h_m + \phi_{\mathrm{mov},mn} + \phi_{\mathrm{offset},mn} \\ &= k_{z,n}\Delta h - (k_{z,m} - k_{z,n})h_n + \phi_{\mathrm{mov},mn} + \phi_{\mathrm{offset},mn} \end{aligned} \quad (1)$$

Δh is related to this observable via the [...]height sensitivity $k_{z,n}$ of interferogram n. [...]In order to estimate Δh, the other terms had to be quantified and removed. The second term is a small residual topographic contribution that we removed using the auxiliary DEM. The third term $\phi_{\mathrm{mov},mn}$ due to the along-track baseline is zero over dry land but can be non-zero over moving water surfaces (see Fig. S2 for details). The fourth term $\phi_{\mathrm{offset},mn}$ is a phase offset e.g. due to orbital errors which changes only slowly across the interferogram. We removed it by mild high-pass filtering [...](Rizzoli et al., 2012) with a length-scale of 600 m that is much larger than the individual thermokarst disturbances. The filtering procedure was robust to outliers as it was based on the median and was not applied to masked pixels like radar shadow or water surfaces. Note that this filtering also largely cancelled [...]seasonal thaw subsidence, which we will generally neglect in the following because of its small magnitude compared to the uncertainties (Günther et al., 2015).

3.1.2 Uncertainties

The uncertainty [...]of the observed height changes [...]were typically between 30-60 cm. As these uncertainties are comparable to the signal magnitude, a detailed uncertainty analysis is required. We estimated the uncertainty from the phase noise, which in turn was estimated from the observed coherence magnitude $|\gamma|$. The coherence magnitude is an indicator of the similarity of the image pair: it takes on values between 0 (no similarity) and 1 (perfect similarity and high phase quality) (Bamler and Hartl, 1998). We employed standard techniques to translate the phase noise inferred from the observed coherence to an uncertainty in Δh [...](see Sec. S1.1 [...]for details).

The coherence magnitude and with it the phase noise are influenced by surface characteristics and measurement properties in several ways. Firstly, a loss of coherence can be induced by the additive measurement noise (Krieger et al., 2007). Secondly, temporal changes between the two acquisitions also reduce the coherence. While this effect is minimized in the single-pass system TanDEM-X, a short effective temporal baseline remains, which is associated with decorrelation over water surfaces. The decorrelation is expected to increase with wind speed: simple modelling further indicated that it may also be relevant over mixed pixels that contain sub-resolution water bodies (Fig. S2a). Finally, the height variability within the resolution cell is associated with geometric decorrelation (Fig. S2b). For extended planar slopes, this can be largely compensated for by spectral filtering, but the impact of vegetation and irregular terrain cannot be cancelled (Krieger et al., 2007). Vegetation also biases the height estimates, i.e. the estimated height will not coincide with the terrain height; we will assess the impact on estimating Δh in the shrub tundra separately when we consider measurement biases.

The coherence-based uncertainty estimates were assessed independently and found to be accurate to within approximately 30% and generally conservative (see Sec. S1.3 for details). The rationale of the assessment was to compare the predicted uncertainty to the observed variability within areas that could be assumed stable and homogeneous (Rizzoli et al., 2012). The analysis of stable areas further allowed us to assess residual biases due to ϕ_{offset}, which were found to be small (2 cm) compared

to the overall uncertainty ([...]>30 cm, Fig. S6). Also the uncertainty due to errors in the input DEM or the orbit information was estimated to be small by comparison. In other words, the phase noise is the limiting factor in the precision of estimated height changes.

The observed height change does not necessarily reflect the true height change within the resolution cell. We found three important sources of bias in the tundra: late-lying snow packs, shrub phenology and water surfaces. The ablation of snow packs induced an apparent lowering of the surface [...]of more than 1 m (Fig. S1), which could be mistaken for thermokarst. Conversely, over tall shrubs the single-pass observations indicated positive elevation changes of several decimetres in June, coincident with leaf-out (C. Wallace, personal communication). Finally, over water bodies, the sign of the measurement bias depended on the wind conditions, [...]and its magnitude exceeded several metres. We believe that the best way to mitigate all these biases is to mask them where necessary. [...]Our focus here is on hillslope thermokarst phenomena, so that open water surfaces were of minor concern. By contrast, snow was a [...]potential error source, at least in June, when late-lying snow patches persisted in many slumps. To assess the role of snow on the measurements, we mapped the presence of snow patches within slumps using medium-resolution satellite imagery in June and July. The details of this analysis, as well as an in-depth assessment of biases can be found in Sec. S1.2.

3.1.3 [...]

[...]

3.2 Mapping of disturbances

To identify and map disturbances in the study regions, we used high to medium resolution optical data. In the Tuktoyaktuk coastlands, we inventoried 160 thaw slumps that showed signs of recent activity with Sentinel-2 imagery from 2016 (10 m visible and near infrared). The slumps were identified based on their distinctive appearance caused by exposed mineral soils and limited vegetation cover, their shape and the presence of a headscarp (Lantuit and Pollard, 2008). In polycyclic slumps [...]we mapped those units that showed signs of recent activity. Within the inventory, all slumps were located in immediate proximity to lakes and their distribution was non-uniform, with higher abundance on morainal deposits (Kokelj et al., 2009). The slump size varied by about two orders of magnitude and could reach up to more than 5 ha (Fig. [...]2a); 14% of the slumps exceeded 1 ha in area, but the median size was considerably smaller (0.4 ha). Slopes of all aspects are affected by slumping, but features with northeast and northwest orientations are more common (Fig. 2b), which is consistent with previous findings by (Kokelj et al., 2009). To further characterize the slumps, we extracted diverse attributes from the satellite image (Normalized Difference Vegetation Index: NDVI) and from topographic data sets (elevation and drainage for the slump centroid from a pre-disturbance DEM, Northwest Territories Centre for Geomatics (2008), local relief as a proxy for headwall height from the TanDEM-X data). To quantify the decadal-scale dynamics, we analysed orthophotos from 2004 (<1 m resolution). For each slump (except one, which was not covered by the aerial imagery), we determined whether the location had not been disturbed in 2004 (14% of the slumps), whether the same slump had already been present and had continued activity (21%), or whether there had been an earlier generation slump (65%). During this time interval, the areal expansion of the slumps was 0.3 ha on

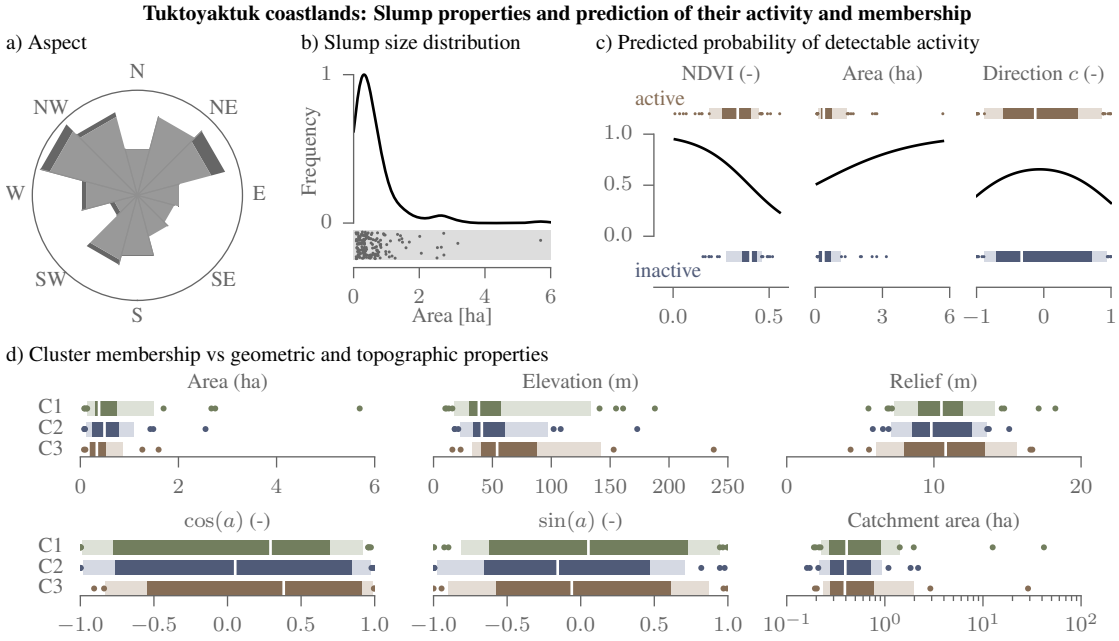

Figure 2. Statistics of thaw slumps in the Tuktoyaktuk coastlands. a) Headwall orientations (darker colour represents slumps whose area exceeds 2 ha); b) Size distribution (histogram and scatter plot); c) Predicted probability of activity plotted with black line for each explanatory variable (all other explanatory variables set to their median) with observed distribution of each variable for the active slumps above and the inactive ones below (white line: median, dark colour: interquartile range, light colour: 10th and 90th percentile, dots: remaining values). The direction factor c is the cosine between look direction and headwall orientation. d) Distribution of topographic and geometric slump properties for all three clusters of sub-seasonal activity C1–C3. a is the headwall aspect.

average for the latter two categories. In addition to the thaw slumps, we also mapped several disturbed shorelines along the Eskimo Lakes, the largest lake in the study region. On the Bykovsky Peninsula and on Kurungnakh Island, we mapped active elongated coastal/riverbank thaw slumps as well as thaw slumps along lake shores.

To quantify the thaw-induced volume losses, we manually delineated active areas within the previously identified thaw slumps in the TanDEM-X data. Despite the clear signal of change in the headwall area of active slumps ([...]see Fig. S8 for an example), constraints associated with the 12 m resolution of the TanDEM-X data have to be considered. The mapped resolution cells may thus also contain undisturbed terrain and scar zone surfaces on either side of the ablating headwall. Thaw slumps were labelled inactive when no [...]volume losses could be detected along the headwall. For the active landforms, representative [...]subseasonal r and seasonal (stacked) r_s volume loss rates were computed by aggregating the TanDEM-X resolution cells within these active parts and forming the median. [...]Their uncertainty is reduced by the aggregation processes and was estimated from the pixel-level uncertainties using parameteric bootstrap analysis (Davison and Hinkley, 1997). Its objective is to mimic the measurement process by generating many potential data sets (aggregate rate estimates) from which the standard error can be estimated; see supplement for details. The measurement process of the aggregate rate depends on

the pixel-level TanDEM-X height changes [...]and their uncertainties. To explore the activity and the subsidence rates of all the inventoried thaw slumps as a function of potential controls such as aspect, we employed logistic regression (activity) and standard regression analysis (r_s). In addition to mapping areas of volume loss along slump headwalls, we also delineated active areas within the scar zones where volume changes could be detected in the TanDEM-X data. These scar zone changes [...]often indicated an elevation gain (Fig. [...]S8), but they were difficult to map because they were generally an order of magnitude smaller than those along the headwall. To compare thaw slump activity with other volume losses, we also estimated volume losses at retreating ice-poor bluffs along the Eskimo Lakes, Tuktoyaktuk coastlands.

3.3 Time-series analysis of sub-seasonal dynamics

To explore and interpret the sub-seasonal dynamics of height changes, we used observations of meteorological parameters. In the Tuktoyaktuk coastlands, we analysed in-situ measurements from Inuvik (precipitation, air temperature, humidity, wind speed and air pressure) and Trail Valley Creek (also incoming and outgoing long and shortwave radiation). Both sites are located in the southern [...]half of the study area at a distance of 45 km. Despite the proximity, the precipitation records did not match well as persistent and large deviations are common ($\approx$ 20 mm per week, or up to 100%; see Fig. [...]S9). Radiation fluxes were also taken from the Ceres SYN1deg-3Hour Ed3A product (incoming shortwave radiation partitioned into direct and diffuse terms), which contains flux estimates from a radiative transfer model and satellite observations (CERES Science Team). The total incoming shortwave radiation and the net longwave radiation compared well with the in-situ measurements (Fig. [...]S9). The Ceres flux data were also employed in the Bykovsky study area, where they were complemented by in-situ meteorological measurements from Tiksi (WMO 21824, 20 km from the study area).

To test the hypothesis that the observed volume losses were energy limited, we estimated headwall ablation using the semi-empirical approach by Lewkowicz (1987). This approach uses meteorological forcing data to estimate the energy available for melting the ground ice by regression formulae that approximate the energy balance modelled using the gradient method for [...]turbulent exchange (input in-situ measurements: air temperature, water vapour pressure, wind speed) and the net radiation (derived from Ceres). The net shortwave radiation was estimated as a function of surface slope and aspect by considering the diffuse and direct incoming radiation and using an albedo of 0.15 for the disturbed slump surface (Lewkowicz, 1987). The hourly estimates of the ablation flux (available energy) were aggregated to estimate the total ablation between two [...]successive TanDEM-X acquisitions (typically 11 days), which could then be compared to the observations. The model predictions have previously been found accurate at daily to monthly time scales, but the model overpredicted the ablation when the ice face was partially covered by debris/snow (Lewkowicz, 1987) in early summer. This early season bias was likely exacerbated by the model's lack of a conductive subsurface heat flux term: the entire ground heat flux is used to melt the ice according to the model, whereas in reality part of the heat flux will warm the cold permafrost. The model further does not consider heat transfer from liquid water, and the representativeness of the forcing data was difficult to ascertain (e.g. unmodelled shading effects, variation of meteorological conditions across the study area). The modelled ablation is sensitive to the ground ice content, which is generally difficult to obtain and also varies across a single slump; we used the value by Lewkowicz (1987). The impact of this assumption was, however, considered small because we focused on the relative temporal variability of the ablation,

not its absolute value. The reason for this is that we measured height changes with 12 m resolution, which were expected to be proportional to the ablation, but whose factor of proportionality remained unknown as it depended on the unknown sub-resolution geometry (e.g. how much of the resolution cell was intersected by the headwall). In addition to this semi-empirical model, we also considered a second reference model of the sub-seasonal dynamics, namely one of uniform rate.

We assessed the consistency of these models with the observations using statistical tests which accounted for the uncertainty of the observations. The null hypothesis of the test was that the time series of height changes were proportional to those predicted by the model. The tests were based on the parametric bootstrapping approach for determining the uncertainties (Davison and Hinkley, 1997): a sample of potential measurements under the null hypothesis was generated and the p-value was computed by determining how extreme the actual observation was compared to this sample (see Sec. S1.5 for details). Small p-values $p < 0.05$ indicated statistically significant deviations from sub-seasonal dynamics that were either uniform or proportional to the energy balance.

To explore the synchronicity of the sub-seasonal dynamics of elevation losses across the Tuktoyaktuk coastlands, we used clustering analysis. The fuzzy c-means clustering approach found representative time series (the clusters) so that the normalized dynamics of the landforms within one cluster were as similar, i.e. the volume loss as synchronous, as possible (Liao, 2005). In addition to the clusters, the analysis produced, for each landform, a degree of membership to all cluster centres; we assigned the landforms to the cluster to which they had the highest membership. The number of clusters was determined using the elbow method (see Sec. S1.6 for details).

4 Results

4.1 Tuktoyaktuk coastlands

In the Tuktoyaktuk coastlands study area, elevation losses were commonly observed in the headwall area of slumps, in contrast to large swathes of the study area which appeared stable. [...]More than half of the inventoried slumps (89/160; Fig. 3a) exhibited detectable activity in the TanDEM-X data. As the activity and its detectability may be influenced by slump characteristics and the sensor viewing geometry, we compared the detected activity to the slump's NDVI, area and its orientation to the satellite sensor using logistic regression (Fig. [...]2c). Smaller NDVI values, indicating sparse vegetation cover, were associated with a higher probability of detected activity. The model predicted a slightly higher chance of detecting activity when the satellite look direction was parallel to the strike of the headscarp ($c = 0$) than when the headwall was observed from behind ($c = 1$; potential shadow) or face-on ($c = -1$; potential layover). The areal extent of a slump was not a useful predictor of detectable activity [...]and neither was the headwall height.

Observed sub-seasonal volume loss rates r at the active slumps varied throughout the summer season, in a way that did not reflect the energy available for ablation. The discrepancy was most pronounced in early summer (early June to mid-July), as volume losses were smaller than in the second half of summer, despite the ample available energy[...]. The largest slump in the study area (152, shown in Fig. 4[...]a) is a case in point, as the volume loss rate is low in early summer. For all slumps covered by the ascending orbit, the median volume loss rate increased from 0 $\mathrm{cm\ d^{-1}}$ in early June to around 3 $\mathrm{cm\ d^{-1}}$ in

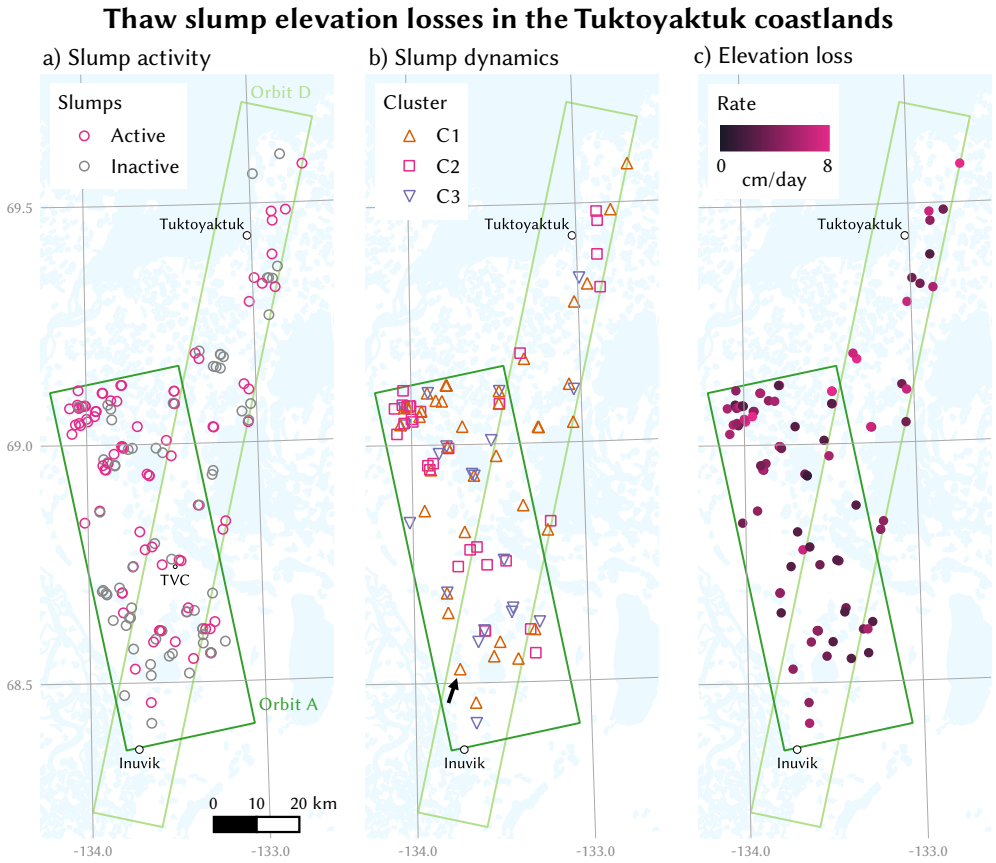

Figure 3. Overview of the study area and all mapped thaw slumps. a) Slumps in the TanDEM-X data according to whether activity could be detected. The locations of in-situ measurements at Inuvik and Trail Valley Creek (TVC) are also shown. b) The sub-seasonal dynamics from mid-July to late August form three clusters. [...]The arrow denotes the [...]slump 152 shown in [...]Fig. [...]4. c) [...]Variability of the seasonal elevation loss [...]rate r_s from mid-July to late August[...].

late July and August [...](Fig. 4b). The acceleration was also evident when looking at the slumps individually as 94% exhibited smaller elevation losses in early June compared to August, indicating the presence of a negative control (e.g. debris cover) on ablation. After all, potential ablation fluxes as predicted using the energy balance approach were highest in June and early July and subsequently dropped by around one quarter. The difference between the sub-seasonal dynamics of the observed volume losses and the hypothesized ablation-driven ones was statistically significant for the majority of slumps (53%; from June to August).

Also in the second half of summer (mid-July to late August), deviations from energy-limited ablation-driven volume losses were commonly observed, as only a subset of the thaw slumps exhibited volume losses that approximately tracked the energy available for ablation. This subset formed one of three distinct categories (as suggested by clustering analysis, see Sec. S1.6), each of which exhibited a large degree of synchronicity. The first cluster C1 corresponded to a fairly steady volume loss, similar

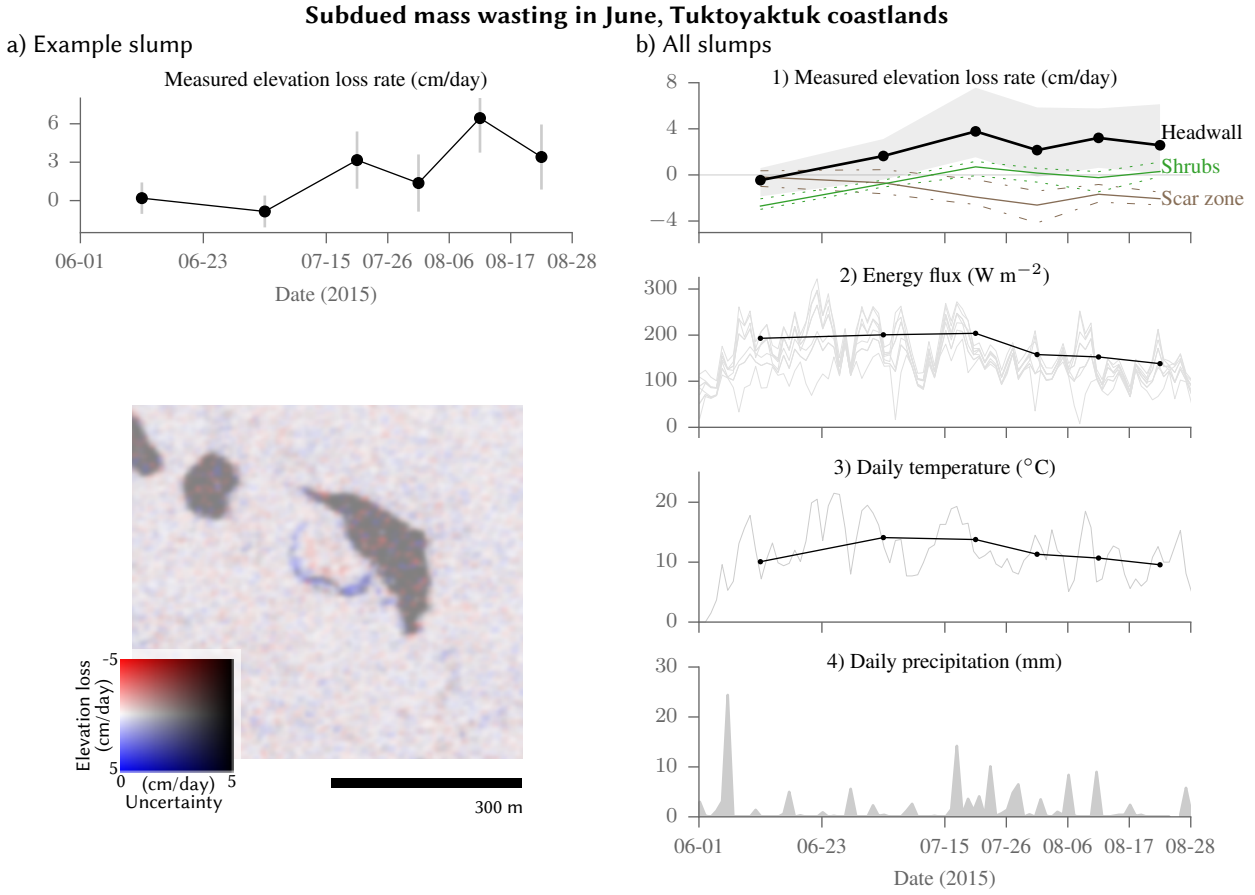

Figure 4. Observed time series of elevation losses [...]in the Tuktoyaktuk coastlands. a) [...]Sub-seasonal elevation loss rates r at thaw slump 152 (see Fig. 3) are lower in June and early July than later in summer. The rates r are plotted halfway between the differenced successive TanDEM-X acquisitions (shown by ticks). The elevation losses occur at the arcuate headwall, as shown below (stacked losses r_s between mid-July and August). b) 1) Spatially aggregated sub-seasonal elevation loss rate r at thaw slumps covered by the ascending orbit ($N = 71$; solid black line: median, grey area: interquartile range), along with observed rates over all slump scar zones with detected changes ($N = 25$) and over patches with dense shrub cover ($N = 10$). The observed elevation loss rate is plotted halfway between the earlier and the later acquisition (indicated by ticks). [...]2) Available energy for different headwall orientations (grey) and temporal averages for a horizontal surface (black). [...]3) Temperature at Inuvik (daily averages in grey; averages between subsequent acquisitions in black). [...]4) Daily precipitation measured in Inuvik. .

to the expected energy-limited trajectory; it contained almost half the slumps (Fig. 5). Conversely, the other two clusters largely exhibited volume losses that did not appear to be controlled by the hypothesized energy-limited variability. Cluster C2 appeared to be related to intense precipitation events recorded at Inuvik in that it showed two peaks in mid-July and mid-August [...](Fig. 5). The degree to which volume losses [...]increased during these two time intervals varied across the slumps. As these peaks were at odds with the smoothly varying available energy from turbulent exchange and radiation, the null hypothesis of ablation-driven volume losses could be rejected more often than for features in cluster C1 (Fig. 5[...]). Finally, less than a quarter of the slumps exhibited an end-of-summer acceleration of subsidence (C3), but a majority of ice-poor lake bluffs did (Fig. 5). As the available energy decreased towards late August, the observed accelerating volume losses were predominantly significantly different from the hypothesized energy-limited trajectories.

Not all landforms fitted neatly into this classification, as certain sub-seasonal dynamics appeared to be mixtures of two clusters or different altogether. A few illustrative examples are shown in Fig. [...]S10a, whereas Figs. [...]S11–S16 show all thaw slumps. The examples include slumps that showed intermittent speed-up in late July (classified as C1) or that accelerated slowly during all of August (classified as C3). Also, negative volume losses (apparent uplift) were commonly observed, but their magnitude was rarely larger than the standard error (only for 7%). One example of an unusual slump is the [...]one previously discussed (152; Fig. 4): it appeared to be a mixture of C1 and C2 in that it speeded up intermittently in mid-August (like C2) but [...]only to a small extent in July (unlike C2). [...]The significant acceleration was observed in the measurements from both orbits and appeared to be limited to around one quarter of the headwall length, illustrating the potential intra-slump variability that the sensor resolution did not allow us to study except for this very large slump [...](Fig. S10b).

The cluster membership and hence the sub-seasonal dynamics were poorly related to the geographical location or easily measured slump characteristics such as the size. All three types of dynamics occurred in the entire study area, often in close proximity (Fig. 3). Neither could they be well distinguished by geometric and topographical properties, as the headscarp aspect, local relief and catchment size were similar for all three clusters (Fig. [...]2d). The slump area and elevation provided some insight, as [...]landforms in cluster C3 – the late speed-up – tend to be smaller and at slightly higher altitudes. Also a comparison with each slump's state in 2004 – for instance whether the location had been undisturbed – did not reveal any clear-cut relation to the cluster membership. Conversely, detectable summer-time height changes in the scar zone were closely related to the cluster membership (Figs. [...]S11–S16), as they were chiefly observed at slumps that responded to strong precipitation events (C2). This association, along with the [...]sign (predominant height increase) and magnitude (decimetres) [...]of the scar-zone elevation change suggests a strong [...]coupling of headwall mass wasting with downstream sediment dynamics at these slumps.

To further explore the spatial variability of the volume losses in the second half of summer, we also investigated the time-averaged volume loss rates r_s (mid-July to late August, 4 TanDEM-X acquisitions). Across all slumps [...]r_s varied typically between 2-5 $\mathrm{cm\ d^{-1}}$ with a weak dependence on location and headscarp geometry (Fig. 6a, both orbits). Regression modelling of r_s in terms of slump properties indicated that south-facing slumps were slightly more active (by $\approx 0.8\ \mathrm{cm\ d^{-1}}$) than north-facing ones (Figs. 6b, [...]S17), which would be consistent with the hypothesized dominance of the available energy (especially insolation). For a given headwall orientation, the elevation loss rates were predicted to increase very little, if at all, with headwall height and slump area. However, the regression could explain little of the observed scatter ($R^2 = 0.14$) and

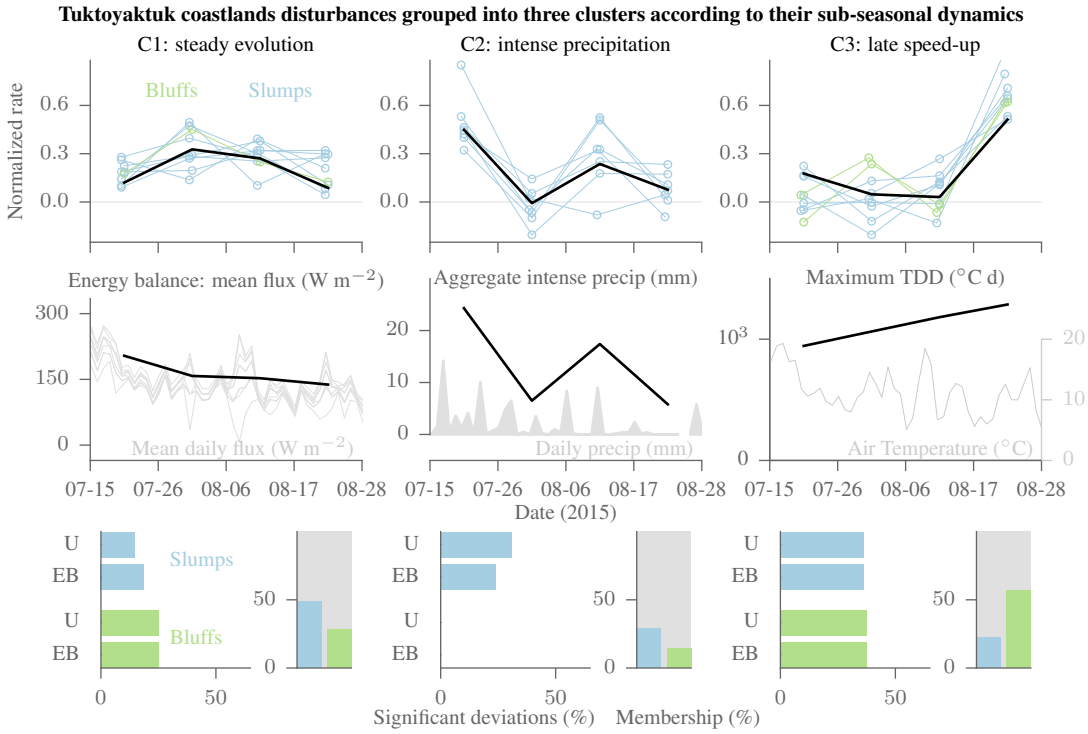

Figure 5. Slumps and bluffs in the Tuktoyaktuk coastlands were grouped into three clusters (C1-C3) according to their sub-seasonal elevation loss dynamics after mid-July. The first row contains the normalized rates of the three clusters (aggregated over the headwall; absolute elevation changes sum to one), with the time series of selected slumps and bluffs shown in blue and green, respectively, and the representative cluster dynamics in black. The second row contains the available energy (grey: daily values for different headwall orientation; black: aggregate values for horizontal orientation); the precipitation (daily values measured in Inuvik in grey, aggregate values for days with intense precipitation $>$ 5mm in black); and the air temperature measured in Inuvik (daily values in grey, maximum thawing degree days TDD between [...]successive acquisitions in black). The third row contains the percentage of landforms for which the null hypothesis of uniform (U) or energy balance-limited (EB) elevation losses was rejected (horizontal bars) and the percentage of landforms that were classified in the respective cluster (vertical bars).

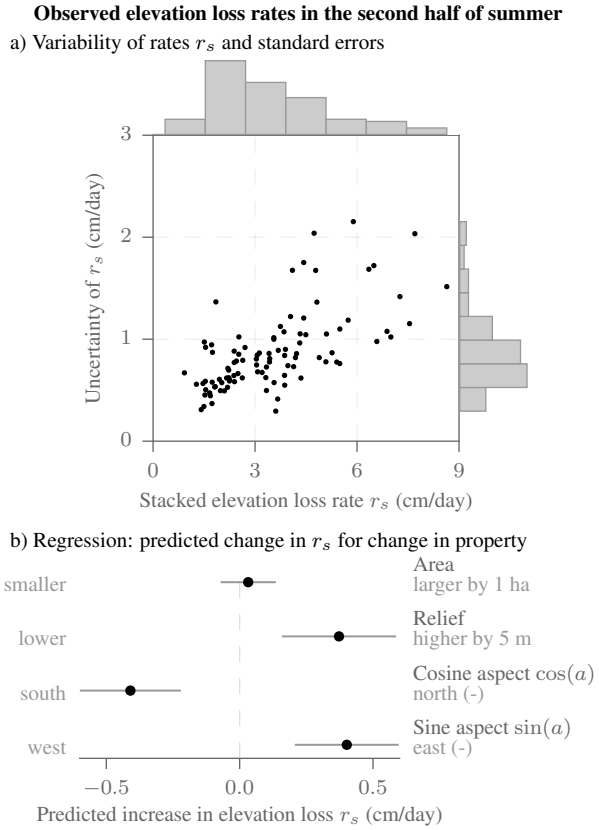

Figure 6. [...]Seasonal elevation loss rates r_s at slumps (both orbits) in the Tuktoyaktuk coastlands, temporally averaged between 15 July and 28 August 2015. a) Scatter plot of r_s estimates and their standard error. b) Dependence of r_s on slump features as predicted by the regression model: the dots show the predicted change in r_s for a change in the property of the annotated magnitude (e.g. 5 m increase in headwall relief), the bars indicate plus/minus one standard error.

the regression coefficients tended to be comparable or smaller in magnitude than their standard errors. [...]Apart from natural variability and the limited precision of the observations, one likely reason for the lack of spatial consistency was the sub-resolution geometry due to which the observed volume losses were related to the headwall retreat by an unknown and spatially variable factor of proportionality.

4.2 Lena River Delta area

On the Bykovsky peninsula, localized volume losses were observed along [...]all coastal thaw slumps, whereas the interior appeared to be stable. Actively retreating thaw-slump yedoma cliffs were detected on both the east coast (favourable viewing geometry) and the west coast (problematic viewing geometry inducing foreshortening, layover). The mean rates of volume loss were similar for cliffs on either coast (3 - 5 $\mathrm{cm\ d^{-1}}$, Fig. 7). So were the sub-seasonal dynamics as all volume loss rates were fairly constant from June to August [...](hence no clustering, Fig. 7). The near-uniform dynamics resembled the available

energy, which changed by only 15% during the summer. However, the similarity of the observations to the hypothesized energy-limited losses may have been misleading in early summer, as the volume losses were likely overestimated before mid-July due to contemporary snow ablation (volume losses were also observed in gullies, and residual snow was still present in early July, see Fig. [...]S18).

The island of Kurungnakh in the Lena Delta was comparatively stable after the ablation of most snow banks (after 11 July, Fig. [...]S19). The only lake-side retrogressive thaw slump in the area did not show any detectable changes. The steep yedoma river-bank slumps on the eastern shore were very poorly imaged because of extreme foreshortening and layover[...]. Consequently, volume losses were detected in only a few spots, despite the known activity of these slumps. The viewing geometry was more favourable at the northern shore, where localized height losses were particularly pronounced in steep gullies. However, we attributed this signal in the gullies largely to snow, as it was most pronounced during mid-July ($\approx 10\mathrm{cm}\ \mathrm{d}^{-1}$) when snow packs were observed to persist in these deep gullies (A. Morgenstern, personal communication). [...]

5 Discussion

5.1 Sub-seasonal mass wasting

Our landscape-scale analyses reveal sub-seasonal patterns of mass wasting that are common to most features, especially the slow onset of ablation in early summer, which suggest the widespread presence of a common control. Conversely, the observed synchronicity of only limited subsets of landforms indicates the presence of distinct processes whose impact is particularly pronounced for only those subsets. [...]

The delayed onset of volume losses in early summer despite the large available energy indicates that mass wasting is not energy limited at this time. Lewkowicz (1987) and Lacelle et al. (2015) observed that early-season mass wasting can veneer late lying snowdrifts, protecting ice-rich permafrost from early-season thawing. Snow cover was still widespread in thaw slumps at the time of the first radar acquisition in early June (Tuktoyaktuk coastlands), but likely limited in depth due to the preceding weeks of above-zero temperatures. [...]Snow had largely disappeared by mid-June (Fig. [...]S20), but subdued [...]elevation losses persisted into July according to the TanDEM-X data, [...]suggesting the importance of debris cover, possibly also on top of snow. In addition, even in the absence of a persistent snowbank, a portion of the available energy must also go into warming cold permafrost behind the slump headwall. However, our data do not allow us to distinguish between these two processes. Conversely, we do not believe the observed early-season signal to be spurious[...], as the snow bias is of the wrong sign. [...]Also the influence of shrubs is too small [...]to explain the reduced volume losses by itself (Sec. S1.2)[...], and it should be negligible in most active slumps, as shrubs are restricted to adjacent disturbed areas within the 12 m resolution cells.

Energy-limited [...]mass wasting appears to have been important from mid-July to late August, as a uniform or slowly decreasing activity was typical. Such mass loss driven by the energy available for ablation has previously been found to govern sub-seasonal rates of headwall retreat in Alaska [...]and on Banks Island, Canada [...](Lewkowicz, 1987; Barnhart, 2013). We observed steady mass wasting at the majority of slumps in the Tuktoyaktuk coastlands (C1), and also at coastal [...]slumps on

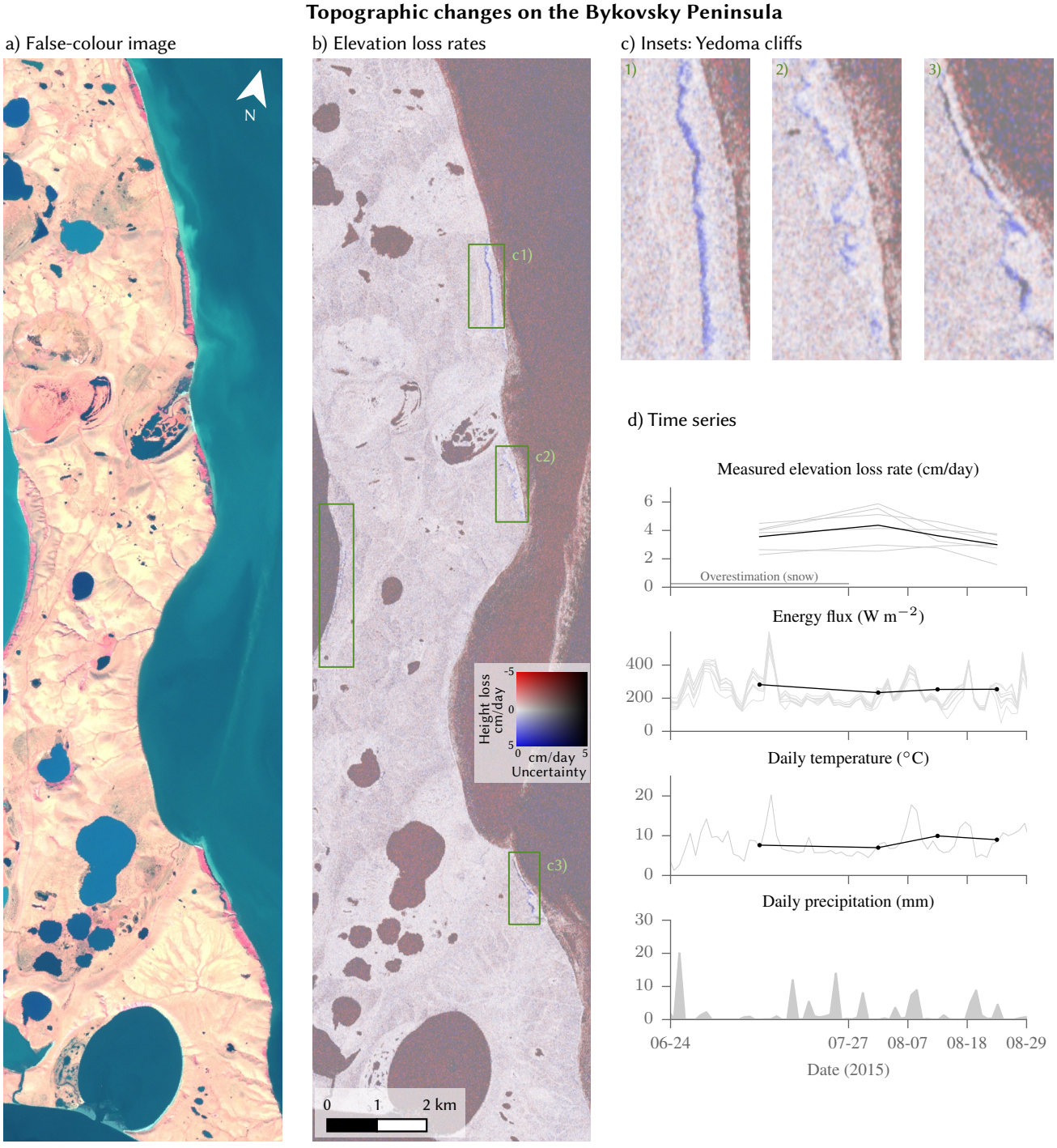

Figure 7. Rapid permafrost degradation occurred at coastal thaw slumps on the Bykovsky Pensinsula. a) Sentinel-2 image. b) Mean elevation loss from 27 July to 28 August 2015 r_s estimated from TanDEM-X is large at yedoma cliff slumps (rectangles). c) Magnified images showing three coastal stretches from b). d) Time series of observed elevation [...]loss rates r at cliffs (aggregated along headwall) and atmospheric conditions similar to Fig. 4, except that the topmost panel shows the dynamics of all cliffs (grey) and their average (black).

the Bykovsky Peninsula. A strong link between sub-seasonal ablation rates on coastal yedoma cliffs and the energy balance has previously been observed on Muostakh Island (15 km south of Bykovsky Peninsula) (Günther et al., 2015). [...]

However, deviations from energy-limited mass wasting were found also in the second half of summer, as increased activity [...]occurred during periods of intense rainfall events. We believe the precipitation-linked volume losses of slumps in cluster C2 (Tuktoyaktuk coastlands) not to be a measurement artefact, as the magnitudes were large compared to the biases that changing soil moisture conditions are expected to induce (cf. Sec. S1.2). Whether precipitation really was the driver is difficult to say because of the short time series, the [...]measurement frequency of 11 days and the lack of agreement among the available precipitation records. [...]It is however not implausible as rainfall could increase volume losses by flowing water delivering extraneous energy to the headwall (Barnhart, 2013; McRoberts and Morgenstern, 1974), or by additional water removing insulating debris accumulation from the headwall and evacuating accumulated sediments from the foot of the headwall and the scar zone [...]via fluidized flow (Burn and Friele, 1989; Kokelj et al., 2015). However, partitioning these effects is difficult as the sensor resolution did not allow us to distinguish headwall retreat from the evacuation of material from the foot of the headwall. [...]The headwall area appeared to be coupled to the scar zone further downstream, as suggested by the commonly observed height changes in the scar zone. However, the temporal patterns in the scar zones were unlikely mono-causal due to their heterogeneity (e.g. Fig. [...]S12). Many slump floors showed increased accumulation (positive height changes) during the periods of increased headwall volume losses while others did not, indicating a non-uniform balance between the increased sediment supply and [...]net accumulation of materials in the scar zone, and the increased capacity for removal following intense rainfall.

The late speed-up characteristic for cluster C3 is also at odds with energy-limited volume losses. Instead, it may point to an increased sensitivity to warming as the warm season becomes longer. The mechanisms are not clear, [...]but a number of processes could give rise to this behaviour. It may be related to an insulating cover that persists for an uncharacteristically long time compared to the majority of thaw slumps[...]. Alternatively, the acceleration could also be due to an internal instability. For instance, ice-poor parts of slump headwalls can fail upon reaching a sufficient thaw depth or when undercut by ablating material underneath (McRoberts and Morgenstern, 1974; Wobus et al., 2011), although this also occurs earlier in the thaw period[...]. A mechanical instability seems particularly plausible for ice-poor bluffs that do not ablate and for which a late speed-up was commonly observed (Fig. 5). However, the slightly larger peak wind speeds in late August (can, 2017) may also contribute by increasing wave-induced erosion, which is likely an important factor for bluff erosion. Irrespective of the origin, the observations highlight the need for detailed observations and modelling efforts to better characterize the vulnerability of permafrost to warmer, longer and stormier summers.

5.2 Single-pass radar interferometry

The spatial variability only becomes evident in synoptic observations, highlighting the importance of remote sensing approaches for understanding and quantifying permafrost degradation. Single-pass interferometry from satellites can offer such large coverage, but it is subject to limitations in terms of precision, spatial resolution and systematic errors. In many ways, we have pushed the TanDEM-X data to their limits, as evidenced by the substantial uncertainties of short-term elevation changes.

The height precision of around 50 cm did not allow for more detailed analyses of changes in the scar zones, and especially for smaller or less active slumps it is comparable to the elevation changes on sub-seasonal time scales. The limited resolution of 12 m is a problem for detecting and observing mass wasting at small slumps. It likely induced sampling biases in this study, as small slumps with little activity were more difficult to capture than the bigger ones like that in Fig. 4. A higher resolution would also be helpful for distinguishing sediment transport near the headwall from headwall backwasting. Systematic errors such as biases induced by the shrub phenology must be considered when using single-pass interferometry data, especially in large-scale analyses where manual masking approaches are insufficient.

In summary, single-pass interferometry with its large and potentially frequent coverage complements more established techniques like airborne LiDAR and spaceborne photogrammetry, which can provide higher resolution and often more accurate elevation measurements. To an even larger degree, it complements detailed field studies of permafrost degradation and its consequences. It is only through a nested approach that small-scale field studies can be put into a regional and continental context by synoptic satellite observations. To achieve this goal, the observational capabilities of earth observation satellites need to be maintained and extended. In this context, single-pass radar observations at higher radar frequencies such as Ku-band, which are currently not available from satellites, seem promising owing to the higher resolution and height precision.

6 Conclusions

This study analysed sub-seasonal dynamics of rapid permafrost thaw in two ice-rich study sites during summer 2015. Our objectives were to map thermokarst activity by observing elevation changes using single-pass interferometry and to analyse the observed sub-seasonal dynamics with respect to their spatial variability and potential drivers of permafrost degradation. Our guiding hypothesis was that mass wasting was limited by the energy required to melt the ground ice on sub-seasonal time scales, so that the 11-day mass losses should track the available energy. Our major findings and conclusions are as follows.

1. The synoptic TanDEM-X single-pass observations revealed spatial variability in rates and in sub-seasonal dynamics of elevation changes which would be difficult to capture with in-situ measurements alone. The observed spatial variability was only poorly explained by macroscale characteristics such as aspect angle, which may indicate the importance of local geomorphic influences such as the [...]ground ice content and soil conditions. Observational limitations also contribute; these are induced by the small magnitude of the elevation changes, which is commonly comparable to the instrument precision, by observational biases and by the limited resolution.

2. During the early thaw period in June, thaw slumps in the Tuktoyaktuk coastlands were less active than the available energy would suggest, indicating the widespread presence of an insulating veneer of debris or snow on the headwalls. In addition, a considerable amount of the ground heat flux [...]has to warm up the ground to the melting point before ablation can proceed more freely later in the summer.

3. Later in the summer, these slumps exhibited divergent but relatively distinct patterns of volume changes. Many showed approximately uniform or slowly decreasing rates, as would be expected based on the available energy, as did the

coastal thaw slump cliffs on Bykovsky, Russia. Other slumps in the Tuktoyaktuk coastlands showed pronounced and synchronous peaks, which for one type were possibly associated with strong precipitation events, coupled to [...]accumulation and downslope removal of sediment in the scar zone. For another type, the peak occurred at the end of the thaw season, suggesting an acceleration of thaw rates in late summer. In summary, thaw slump mass wasting was not consistently limited by the available energy on approximately weekly time scales.

4. The observed spatial and temporal heterogeneity of thaw slump mass wasting should be considered when predicting thermokarst rates across spatial and temporal scales. [...]The spatial and within-season variability has important implications for estimating the fate of the mobilized carbon, nutrients and sediments. The associated differences in exposure, lateral transport and re-burial of the thawed material deserve further attention[...]. Also, they illustrate the need for nested approaches linking local field investigation with remote sensing to quantify cryospheric change and its consequences across the landscape.

Acknowledgements. The authors thank Annett Bartsch, Birgit Heim and Anne Morgenstern for constructive discussions. Support by the Helmholtz Association (HA310 Remote Sensing and Earth System Dynamics) and by the European Space Agency (SP-InSARAP) is gratefully acknowledged. The TanDEM-X data were provided by DLR through proposal XTI_GEOL6759.

Data availability. The thaw slump inventories and the elevation change estimates have been made available https://doi.org/10.1594/PANGAEA.877506. Intermediate products described in the manuscript are available from the authors upon request. Information on how to obtain the TanDEM-X CoSSc data can be found at https://tandemx-science.dlr.de/.

Competing interests. The authors declare no conflict of interest.

References

Canadian Climate Normals 1981-2010 Station Data, climate.weather.gc.ca, 2017.

Aylsworth, J. M., Burgess, M. M., Desrochers, D. T., Duk-Rodkin, A., Robertson, T., and Traynor, J. A.: Surficial geology, subsurface materials, and thaw sensitivity of sediments, in: The Physical Environment of the Mackenzie Valley, Northwest Territories: A Base Line for the Assessment of Environmental Change, vol. 547, pp. 41–48, Geological Survey of Canada, 2000.

Balser, A. W., Jones, J. B., and Gens, R.: Timing of retrogressive thaw slump initiation in the Noatak Basin, northwest Alaska, USA, Journal of Geophysical Research: Earth Surface, 119, 1106–1120, https://doi.org/10.1002/2013JF002889, 2013JF002889, 2014.

Bamler, R. and Hartl, P.: Synthetic aperture radar interferometry, Inverse Probl., 14, 1–54, 1998.

Barnhart, T.: Morphodynamics of the Selawik Retrogressive Thaw Slump, Northwest Alaska, Master's thesis, Idaho State University, 2013.

Boike, J., Kattenstroth, B., Abramova, K., Bornemann, N., Chetverova, A., Fedorova, I., Fröb, K., Grigoriev, M., Grüber, M., Kutzbach, L., Langer, M., Minke, M., Muster, S., Piel, K., Pfeiffer, E.-M., Stoof, G., Westermann, S., Wischnewski, K., Wille, C., and Hubberten, H.-W.: Baseline characteristics of climate, permafrost and land cover from a new permafrost observatory in the Lena River Delta, Siberia (1998-2011), Biogeosciences, 10, 2105–2128, 2013.

Bowden, W. B., Gooseff, M. N., Balser, A., Green, A., Peterson, B. J., and Bradford, J.: Sediment and nutrient delivery from thermokarst features in the foothills of the North Slope, Alaska: Potential impacts on headwater stream ecosystems, Journal of Geophysical Research: Biogeosciences, 113, https://doi.org/10.1029/2007JG000470, g02026, 2008.

Burn, C.: The thermal regime of a retrogressive thaw slump near Mayo, Yukon Territory, Canadian Journal of Earth Sciences, 37, 967–981, 2000.

Burn, C. and Friele, P.: Geomorphology, Vegetation Succession, Soil Characteristics and Permafrost in Retrogressive Thaw Slumps near Mayo, Yukon Territory, Arctic, 42, 31–40, 1989.

Burn, C. and Lewkowicz, A.: Canadian Landform Examples – Retrogressive Thaw Slumps, Canadian Geographer / Le Géographe canadien, 34, 273–276, https://doi.org/10.1111/j.1541-0064.1990.tb01092.x, http://dx.doi.org/10.1111/j.1541-0064.1990.tb01092.x, 1990.

Burn, C. R. and Kokelj, S. V.: The Environment and Permafrost of the Mackenzie Delta Area, Permafrost and Periglacial Processes, 20, 83–105, 2009.

CERES Science Team: https://doi.org/doi:10.5067/Terra+Aqua/CERES/SYN1deg3HOUR_L3.003A.

Davison, A. C. and Hinkley, D. V.: Bootstrap Methods and their Application, Cambridge University Press, 1997.

Grosse, G., Schirrmeister, L., Siegert, C., Kunitsky, V., Slagoda, E., Andreev, A., and Dereviagyn, A.: Geological and geomorphological evolution of a sedimentary periglacial landscape in Northeast Siberia during the Late Quaternary, Geomorphology, 86, 25 – 51, https://doi.org/http://dx.doi.org/10.1016/j.geomorph.2006.08.005, 2007.

Grosse, G., Harden, J., Turetsky, M., McGuire, A., Camill, P., Tarnocai, C., Frolking, S., Schuur, E. A. G., Jorgenson, T., Marchenko, S., Romanovsky, V., Wickland, K., French, N., Waldrop, M., Bourgeau-Chavez, L., and Striegl, R.: Vulnerability of high-latitude soil organic carbon in North America to disturbance, Journal of Geophysical Research: Biogeosciences, 116, G00K06, https://doi.org/10.1029/2010JG001507, 2011.

Günther, F., Overduin, P. P., Sandakov, A. V., Grosse, G., and Grigoriev, M. N.: Short- and long-term thermo-erosion of ice-rich permafrost coasts in the Laptev Sea region, Biogeosciences, 10, 4297–4318, https://doi.org/10.5194/bg-10-4297-2013, 2013.

Günther, F., Overduin, P. P., Yakshina, I. A., Opel, T., Baranskaya, A. V., and Grigoriev, M. N.: Observing Muostakh disappear: permafrost thaw subsidence and erosion of a ground-ice-rich island in response to arctic summer warming and sea ice reduction, The Cryosphere, 9, 151–178, https://doi.org/10.5194/tc-9-151-2015, 2015.

Jones, B. M., Stoker, J. M., Gibbs, A. E., Grosse, G., Romanovsky, V. E., Douglas, T. A., Kinsman, N. E. M., and Richmond, B. M.: Quantifying landscape change in an arctic coastal lowland using repeat airborne LiDAR, Environmental Research Letters, 8, 045 025, 2013.

Jorgenson, M. T.: Thermokarst Terrains, in: Treatise on Geomorphology, edited by Shroder, J. F., pp. 313 – 324, Academic Press, San Diego, https://doi.org/http://dx.doi.org/10.1016/B978-0-12-374739-6.00215-3, 2013.

Kanevskiy, M., Shur, Y., Strauss, J., Jorgenson, T., Fortier, D., Stephani, E., and Vasiliev, A.: Patterns and rates of riverbank erosion involving ice-rich permafrost (yedoma) in northern Alaska, Geomorphology, 253, 370 – 384, https://doi.org/http://dx.doi.org/10.1016/j.geomorph.2015.10.023, 2016.

Kokelj, S., Tunnicliffe, J., Lacelle, D., Lantz, T., Chin, K., and Fraser, R.: Increased precipitation drives mega slump development and destabilization of ice-rich permafrost terrain, northwestern Canada, Global and Planetary Change, 129, 56 – 68, https://doi.org/http://dx.doi.org/10.1016/j.gloplacha.2015.02.008, 2015.

Kokelj, S. V., Lantz, T. C., Kanigan, J., Smith, S. L., and Coutts, R.: Origin and polycyclic behaviour of tundra thaw slumps, Mackenzie Delta region, Northwest Territories, Canada, Permafrost and Periglacial Processes, 20, 173–184, https://doi.org/10.1002/ppp.642, 2009.

Kokelj, S. V., Lacelle, D., Lantz, T. C., Tunnicliffe, J., Malone, L., Clark, I. D., and Chin, K. S.: Thawing of massive ground ice in mega slumps drives increases in stream sediment and solute flux across a range of watershed scales, Journal of Geophysical Research: Earth Surface, 118, 681–692, https://doi.org/10.1002/jgrf.20063, http://dx.doi.org/10.1002/jgrf.20063, 2013.

Kokelj, S. V., Lantz, T. C., Tunnicliffe, J., Segal, R., and Lacelle, D.: Climate-driven thaw of permafrost preserved glacial landscapes, northwestern Canada, Geology, 45, 371–374, https://doi.org/10.1130/G38626.1, 2017a.

Kokelj, S. V., Palmer, M. J., Lantz, T. C., and Burn, C. R.: Ground Temperatures and Permafrost Warming from Forest to Tundra, Tuktoyaktuk Coastlands and Anderson Plain, NWT, Canada, Permafrost and Periglacial Processes, pp. n/a–n/a, https://doi.org/10.1002/ppp.1934, 2017b.

Krieger, G., Moreira, A., Fiedler, H., Hajnsek, I., Werner, M., Younis, M., and Zink, M.: TanDEM-X: A Satellite Formation for High-Resolution SAR Interferometry, IEEE Transactions on Geoscience and Remote Sensing, 45, 3317–3340, 2007.

Kubanek, J., Westerhaus, M., and Heck, B.: TanDEM-X Time Series Analysis Reveals Lava Flow Volume and Effusion Rates of the 2012-2013 Tolbachik, Kamchatka Fissure Eruption, Journal of Geophysical Research: Solid Earth, 122, 7754–7774, https://doi.org/10.1002/2017JB014309, http://dx.doi.org/10.1002/2017JB014309, 2017JB014309, 2017.

Lacelle, D., Brooker, A., Fraser, R., and Kokelj, S.: Distribution and growth of thaw slumps in the Richardson Mountains-Peel Plateau region, northwestern Canada, Geomorphology, 235, 40 – 51, https://doi.org/http://dx.doi.org/10.1016/j.geomorph.2015.01.024, 2015.

Lantuit, H. and Pollard, W.: Fifty years of coastal erosion and retrogressive thaw slump activity on Herschel Island, southern Beaufort Sea, Yukon Territory, Canada, Geomorphology, 95, 84 – 102, https://doi.org/http://dx.doi.org/10.1016/j.geomorph.2006.07.040, 2008.

Lantuit, H., Atkinson, D., Overduin, P., Grigoriev, M., Rachold, V., Grosse, G., and Hubberten, H.-W.: Coastal erosion dynamics on the permafrost-dominated Bykovsky Peninsula, north Siberia, 1951-2006, Polar Research, 30, 2011.

Lewkowicz, A. G.: Headwall retreat of ground-ice slumps, Banks Island, Northwest Territories, Canadian Journal of Earth Sciences, 24, 1077–1085, https://doi.org/10.1139/e87-105, 1987.

Liao, W. T.: Clustering of time series data—a survey, Pattern Recognition, 38, 1857–1874, 2005.

Littlefair, C. A., Tank, S. E., and Kokelj, S. V.: Retrogressive thaw slumps temper dissolved organic carbon delivery to streams of the Peel Plateau, NWT, Canada, Biogeosciences, 14, 5487–5505, https://doi.org/10.5194/bg-14-5487-2017, 2017.

Liu, L., Schaefer, K. M., Chen, A. C., Gusmeroli, A., Zebker, H. A., and Zhang, T.: Remote sensing measurements of thermokarst subsidence using InSAR, Journal of Geophysical Research: Earth Surface, 120, 1935–1948, https://doi.org/10.1002/2015JF003599, 2015JF003599, 2015.

McRoberts, E. and Morgenstern, N.: The Stability of Thawing Slopes, Canadian Geotechnical Journal, 11, 447–464, 1974.

Morgenstern, A., Grosse, G., Günther, F., Fedorova, I., and Schirrmeister, L.: Spatial analyses of thermokarst lakes and basins in Yedoma landscapes of the Lena Delta, The Cryosphere, 5, 849–867, https://doi.org/10.5194/tc-5-849-2011, 2011.

Northwest Territories Centre for Geomatics: MVAP DEM, http://www.geomatics.gov.nt.ca/, 2008.

Obu, J., Lantuit, H., Grosse, G., Guenther, F., Sachs, T., Helm, V., and Fritz, M.: Coastal erosion and mass wasting along the Canadian Beaufort Sea based on annual airborne LiDAR elevation data, Geomorphology, pp. –, https://doi.org/http://dx.doi.org/10.1016/j.geomorph.2016.02.014, 2016.

Rizzoli, P., Bräutigam, B., Kraus, T., Martone, M., and Krieger, G.: Relative height error analysis of TanDEM-X elevation data, ISPRS Journal of Photogrammetry and Remote Sensing, 73, 30 – 38, https://doi.org/http://dx.doi.org/10.1016/j.isprsjprs.2012.06.004, 2012.

Schirrmeister, L., Schwamborn, G., Overduin, P. P., Strauss, J., Fuchs, M. C., Grigoriev, M., Yakshina, I., Rethemeyer, J., Dietze, E., and Wetterich, S.: Yedoma Ice Complex of the Buor Khaya Peninsula (southern Laptev Sea), Biogeosciences, 14, 1261–1283, https://doi.org/10.5194/bg-14-1261-2017, 2017.

Vonk, J. and Gustafsson, O.: Permafrost-carbon complexities, Nature Geoscience, 6, 675–676, 2013.

Westermann, S., Langer, M., Boike, J., Heikenfeld, M., Peter, M., Etzelmüller, B., and Krinner, G.: Simulating the thermal regime and thaw processes of ice-rich permafrost ground with the land-surface model CryoGrid 3, Geoscientific Model Development, 9, 523–546, https://doi.org/10.5194/gmd-9-523-2016, https://www.geosci-model-dev.net/9/523/2016/, 2016.

Wetterich, S., Kuzmina, S., Andreev, A., Kienast, F., Meyer, H., Schirrmeister, L., Kuznetsova, T., and Sierralta, M.: Palaeoenvironmental dynamics inferred from late Quaternary permafrost deposits on Kurungnakh Island, Lena Delta, Northeast Siberia, Russia, Quaternary Science Reviews, 27, 1523 – 1540, https://doi.org/http://dx.doi.org/10.1016/j.quascirev.2008.04.007, 2008.

Wobus, C., Anderson, R., Overeem, I., Matell, N., Clow, G., and Urban, F.: Thermal Erosion of a Permafrost Coastline: Improving Process-Based Models Using Time-Lapse Photography, Arctic, Antarctic, and Alpine Research, 43, 474–484, 2011.

Wolfe, S. A., Dallimore, S. R., and Solomon, S. M.: Coastal Permafrost Investigations Along a Rapidly Eroding Shoreline, Tuktoyaktuk, N..W.T, in: Prooceedings of the Seventh International Conference on Permafrost in Yellowknife, pp. 1125–1131, 1998.

Zwieback, S., Liu, X., Antonova, S., Heim, B., Bartsch, A., Boike, J., and Hajnsek, I.: A Statistical Test of Phase Closure to Detect Influences on DInSAR Deformation Estimates Besides Displacements and Decorrelation Noise: Two Case Studies in High-Latitude Regions, IEEE Transactions on Geoscience and Remote Sensing, 54, 5588–5601, https://doi.org/10.1109/TGRS.2016.2569435, 2016.